SCIENCE CHINA
Information Sciences

• RESEARCH PAPER •

September 2024, Vol. 67, Iss. 9, 192301:1–192301:17
https://doi.org/10.1007/s11432-024-4066-7

Achieving full mutualism with massive passive devices for multiuser MIMO symbiotic radio

Jingran XU[1], Zhuoyin DAI[1], Yong ZENG[1,2*], Shi JIN[1] & Tao JIANG[3]

[1]*National Mobile Communications Research Laboratory, Southeast University, Nanjing* 210096*, China;*
[2]*Purple Mountain Laboratories, Nanjing* 211111*, China;*
[3]*Research Center of 6G Mobile Communications, School of Cyber Science and Engineering, and Wuhan National Laboratory for Optoelectronics, Huazhong University of Science and Technology, Wuhan* 430074*, China*

Received 5 March 2024/Revised 20 May 2024/Accepted 6 June 2024/Published online 15 August 2024

Abstract Symbiotic radio (SR) is one of the attractive communication technologies to facilitate large-scale Internet of Things (IoT) connections with enhanced energy and spectrum efficiency, where passive backscatter devices (BDs) modulate their information over the radio frequency (RF) signals emitted by the active primary transmitters (PTs). Meanwhile, the primary transmission can be strengthened with the additional multipaths created by BDs. To capitalize to a greater extent on the mutualism relationship between the two types of communication, this paper studies multiple-input multiple-output (MIMO) SR communication systems including multiple PTs and massive BDs. We derive the achievable rate expressions of each PT and BD, as well as the sum rate expressions of primary and secondary communication, respectively. Then asymptotic analysis is given to derive the active and passive communication rates with a large number of BDs. Furthermore, for the general case with a finite number of BDs, we study the precoding optimization problem to maximize the sum rate of primary communication, while ensuring that the sum rate of secondary communication and the individual rate for each PT and BD in the prescribed active and passive user sets satisfy the specified thresholds. Simulation results are presented to verify the analytical studies.

Keywords multiuser MIMO SR, backscattering, massive backscatter devices, asymptotic analysis, active and passive communication

1 Introduction

Internet of Things (IoT) has become one of the critical application paradigms for the fifth-generation (5G) and future wireless communication systems [1–6]. IoT equipment has stringent constraints on cost, energy, and signal processing complexity in practice, hence there is strong necessity to develop communication technologies with high spectrum and energy efficiency for the continuous advancement of IoT [7–9]. Recently, symbiotic radio (SR) has emerged as an appealing option to satisfy such demands with two transmission types: the primary transmission for active devices and the secondary transmission for passive devices. On the one hand, SR enables the passive secondary backscatter devices (BDs) to modulate their information symbols by backscattering the radio-frequency (RF) signals from active primary transmitters (PTs) without requiring expensive and energy-intensive RF chains [10, 11]. On the other hand, SR needs not to occupy additional spectrum since the two types of transmissions share the same spectrum [12, 13]. Due to its ability to integrate with various technologies such as reconfigurable intelligent surface (RIS) [14, 15] and non-orthogonal multiple access (NOMA) [16, 17], SR has received significant attention.

Based on the relation of the symbol rates of the primary and secondary signals, SR can be divided into two categories, including parasite symbiotic radio (PSR), where their symbol rates are equal, and commensal symbiotic radio (CSR), where the symbol rate of primary signals is significantly higher than that of the BD signals [18]. In PSR, the backscattering links are considered interference to the primary links, while in CSR, they create additional paths that can enhance the primary communication. Thus,

* Corresponding author (email: yong_zeng@seu.edu.cn)

© Science China Press 2024

the mutual benefits can be achieved for both transmission types in CSR. Ref. [19] analyzed the condition on the relative symbol duration ratio between primary and secondary transmissions, so that the two can benefit each other in SR. Based on simulations, Ref. [11] demonstrated the enhancement to primary transmission from the backscattering link when it is sufficiently strong.

There are some preliminary studies on SR with multiple BDs [20–27]. For example, Ref. [20] employed deep reinforcement learning (DRL) to attach every BD to a suitable cellular user when investigating the user association issue in SR networks. The transceiver design in multi-BD SR systems is studied in [21] by using stochastic optimization methods. To mitigate the interference between multiple BDs, multiple access techniques for SR systems are studied in [22–25]. Refs. [26, 27] compared the spatial division multiple access (SDMA) scheme with the dynamic time division multiple access (TDMA) scheme and the selection diversity access (SDA) scheme in SR systems, and it is shown that compared to the other two schemes, SDMA can achieve superior performance with a sufficiently large number of BDs. Note that in [26], the backscattering links in CSR are considered as interference, and in [27], the BS, BDs, and receiver are all assumed to have a single antenna.

Owing to the double-hop signal attenuation and backscattering loss involved, the backscattering link of one single BD is usually very weak compared to the direct link. Thus, SR with single BD or single-antenna terminals is difficult to provide significant performance enhancement to the primary communication. To tackle such problems, Refs. [14, 15] introduced RIS as a BD into SR systems. However, since RIS usually has massive reflecting elements that require dynamic phase manipulations, it may incur high signaling and maintenance costs, which make it difficult to deploy for those low-cost IoT devices that have small form factors. Inspired by the vision of 6G to support ultra-massive scale connectivity, in [28], we propose to significantly augment secondary backscattering links by exploiting the multipath gains from a large number of BDs to achieve full mutualism of SR. Specifically, massive BDs can not only offer rich multi-user diversities for passive secondary backscattering transmission, but also provide significant multipath gains to enhance the active primary communication. Note that SRs with massive BDs or RIS can be applied to two different and complementary scenarios. In multi-BD-based SR, each BD has independent information communication requirements. By contrast, for RIS-based SR, an RIS that is composed of a large number of passive reflecting elements corresponds to one secondary information source only.

Note that in [28], only one PT was considered and the asymptotic analysis of the relationship between two types of communication rates was given by assuming the PT has a single antenna. In this paper, a more general SR system with multiple PTs and massive BDs is investigated. Our main contributions are summarized as follows.

- First, we study a multiuser multiple-input multiple-output (MIMO) SR system with massive BDs, where a general model to fully exploit the mutualism relationship between active primary users and passive BDs is established. We then derive the achievable rate expression of each PT and BD, as well as the sum rate expressions of primary and secondary communication, respectively, by using the minimum mean square error estimation (MMSE) receiver with successive interference cancellation (SIC), since both primary and secondary systems correspond to an equivalent multiple access channel (MAC).
- Next, to reveal the effect of the number of BDs on the communication rates of SR, we analyze the asymptotic performance with large-scale BDs. Closed-form expressions for the sum of primary and secondary communication rates are derived respectively, both of which are demonstrated to increase with the number of BDs and PTs. Furthermore, the transmit precoding optimization problems to maximize the individual primary and secondary asymptotic rates are formulated and solved, and it turns out that the two problems correspond to the same optimal solution. This demonstrates that a win-win situation for both primary and secondary communication could be achieved for SR with massive BDs.
- Furthermore, for the general case with a finite number of BDs, we formulate a precoding optimization problem to maximize the sum rate of primary communication, while ensuring that the sum secondary communication rate and the communication rate for each PT and BD in the prescribed user sets are no smaller than the specified thresholds. The original problem is non-convex, and we apply an effective technique to transform the optimization variables into the transmit covariance matrices of PTs, based on which an equivalent problem is obtained. We then propose an effective solution based on successive convex approximation (SCA) technique. Numerical results are given to validate our theoretical analysis.

The rest of this paper is organized as follows. Section 2 introduces the system model of multiuser and multi-BD-based MIMO SR communication. In Section 3, the achievable rate of the individual and the sum primary active users and secondary BDs are derived respectively. In addition, the asymptotic performance of primary and secondary communication is analyzed and closed-form expressions are derived

Table 1 List of notations used in this paper

Parameter	Value	Parameter	Value
M	The number of PTs	$\boldsymbol{s}_m(l,n) \in \mathbb{C}^{N_m \times 1}$	The information-bearing symbols of PT m
K	The number of BDs	$c_k(n) \in \mathbb{C}$	The information-bearing symbols of BD k
N_t	The number of antennas of each PT	α	Power reflection coefficient
N_r	The number of antennas of the AP	P_m	Transmit power of PT m
L	Ratio between symbol duration of the BDs to the PTs	$\boldsymbol{F}_m$	Transmit precoding matrix of PT m
$\boldsymbol{H}_m$	Channel coefficient from PT m to the AP	σ^2	Noise power
$\boldsymbol{h}_{m,k}$	Channel coefficient from PT m to BD k	$\boldsymbol{H}_{\mathrm{eq},m}$	Equivalent MIMO channel
$\boldsymbol{g}_k$	Channel coefficient from BD k to the AP	$\boldsymbol{W}_m$	Receive beamforming matrix of PT m

with massive BDs. Section 4 studies the precoding optimization problem with the objective to maximize the sum rate of primary communication while ensuring that the sum rate of secondary communication and the individual rate for each PT and BD in the prescribed user sets are no smaller than certain thresholds. Numerical results are given in Section 5 and finally Section 6 concludes the paper.

Notations. In this paper, scalars, vectors and matrices are denoted by italic letters, boldface lower- and upper-case letters, respectively. The Euclidean norm, transpose, and hermitian transpose of a vector $\boldsymbol{x}$ are represented as $\|\boldsymbol{x}\|$, $\boldsymbol{x}^{\mathrm{T}}$ and $\boldsymbol{x}^{\mathrm{H}}$, respectively. For a matrix $\boldsymbol{X}$, the transpose, conjugate, hermitian transpose, Frobenius norm and rank are represented as $\boldsymbol{X}^{\mathrm{T}}$, $\boldsymbol{X}^*$, $\boldsymbol{X}^{\mathrm{H}}$, $\|\boldsymbol{X}\|_F$ and $\mathrm{rank}(\boldsymbol{X})$, respectively. $\mathrm{vec}(\boldsymbol{X})$ denotes stacking the columns of matrix $\boldsymbol{X}$ into a column vector. For a square matrix $\boldsymbol{A}$, $|\boldsymbol{A}|$, $\mathrm{tr}(\boldsymbol{A})$, and $\boldsymbol{A}^{-1}$ denote its determinant, trace, and matrix inverse, respectively, while $\boldsymbol{A} \succeq 0$ represents that the matrix $\boldsymbol{A}$ is positive semidefinite. $\otimes$ refers to the Kronecker product. $\mathrm{diag}(y_1, \ldots, y_N)$ denotes an $N \times N$ diagonal matrix with $y_1, \ldots, y_N$ being the diagonal elements. $\boldsymbol{O}_{M\times N}$ represents the $M \times N$ all-zero matrix. $\boldsymbol{I}_N$ represents an N-dimensional identity matrix. $\mathbb{C}^{M\times N}$ represents the space of $M \times N$ matrices with complex entries. $\mathcal{CN}(\boldsymbol{m}, \boldsymbol{\Sigma})$ denotes the distribution of a circularly symmetric complex Gaussian (CSCG) random vector with mean $\boldsymbol{m}$ and covariance matrix $\boldsymbol{\Sigma}$. In addition, the expectation for the random variable Z is denoted as $\mathbb{E}_Z[\cdot]$. The logarithm with base 2 is represented by $\log_2(\cdot)$.

The notations used in this paper are listed in Table 1.

2 System model

Figure 1 depicts the multiuser MIMO SR system considered in this paper, with M PTs, K BDs and one access point (AP). Each PT and the AP have N_t and N_r antennas, respectively, and each BD has one antenna. Without loss of generality, we assume $N_t \leqslant N_r$. Via backscattering the RF signals from the M PTs, the K BDs can modulate their information without using additional spectrum or power. In return, the scattered signals of BDs can create additional channel paths to strengthen the primary transmission when their symbol duration is significantly longer than that of the signals of PTs, which is the so-called mutualism relationship in SR [29]. Let $\boldsymbol{H}_m \in \mathbb{C}^{N_r\times N_t}$ denote the direct-link MIMO channel from PT m to the AP. Further let $\boldsymbol{h}_{m,k} \in \mathbb{C}^{N_t\times 1}$ denote the multiple-input single-output (MISO) channel from PT m to BD k, and $\boldsymbol{g}_k \in \mathbb{C}^{N_r\times 1}$ denote the single-input multiple-output (SIMO) channel from BD k to the AP. The corresponding cascaded channel from PT m to the AP via BD k is thus denoted as $\boldsymbol{g}_k\boldsymbol{h}_{m,k}^{\mathrm{H}}$.

We consider the setup of CSR [18], in which the symbol rate of the M PTs is $L \gg 1$ times that of the K BDs. Denote the independent and identically distributed (i.i.d.) information-bearing symbols of PT m and BD k as $\boldsymbol{s}_m(l,n) \in \mathbb{C}^{N_m\times 1}$ and $c_k(n) \in \mathbb{C}$, respectively, both of which follow CSCG distribution with normalized power, i.e., $\boldsymbol{s}_m(l,n) \sim \mathcal{CN}(\boldsymbol{0}, \boldsymbol{I}_{N_m})$, $l = 1, \ldots, L$, and $c_k(n) \sim \mathcal{CN}(0,1)$, $k = 1, \ldots, K$. Notice that $N_m \leqslant N_t$ is one of the optimization variables denoting the number of data streams of the signal of PT m that will be optimized later. In addition, denote the transmit power of PT m as P_m, the power reflection coefficient of each BD as $\alpha \in [0,1]$, and the transmit precoding matrix of PT m as $\boldsymbol{F}_m \in \mathbb{C}^{N_t\times N_m}$, satisfying $\mathrm{tr}(\boldsymbol{F}_m\boldsymbol{F}_m^{\mathrm{H}}) \leqslant 1$. The synchronization issue for BDs can be addressed by employing SyncScatter tags proposed in [30], which can achieve accurate synchronization with incident signals at the IoT device level while realizing the maximum possible sensitivity afforded by a backscatter

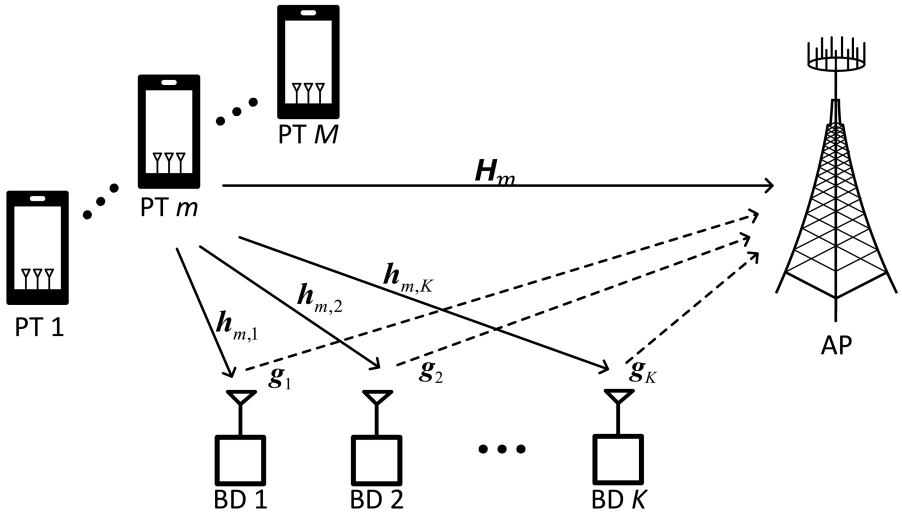

Figure 1 Multiuser MIMO SR with multiple PTs and massive BDs.

link budget. Thus, the received signal at the AP is

$$\boldsymbol{y}(l,n)=\sum_{m=1}^{M}\sqrt{P_m}\boldsymbol{H}_m\boldsymbol{F}_m\boldsymbol{s}_m(l,n)+\sum_{m=1}^{M}\sum_{k=1}^{K}\sqrt{P_m}\sqrt{\alpha}\boldsymbol{g}_k\boldsymbol{h}_{m,k}^{\mathrm{H}}\boldsymbol{F}_m\boldsymbol{s}_m(l,n)c_k(n)+\boldsymbol{u}(l,n),\quad l=1,\ldots,L, \tag{1}$$

where $\boldsymbol{u}(l,n)\in\mathbb{C}^{N_r\times 1}$ denotes the i.i.d. CSCG noise with zero mean and power σ^2, i.e., $\boldsymbol{u}(l,n)\sim\mathcal{CN}\left(\boldsymbol{0},\sigma^2\boldsymbol{I}_{N_r}\right)$.

3 Achievable rate and asymptotic analysis

3.1 Achievable rate analysis

When decoding the PT signals $\boldsymbol{s}_m(l,n)$, the second term in (1) can be seen as the additional multi-path channel components since the BD symbols $c_k(n)$ stay constant for every block of L PT symbols. Therefore, the equivalent MIMO channel for decoding $\boldsymbol{s}_m(l,n)$ depends on the composite BD symbols $\boldsymbol{c}(n)=[c_1(n),c_2(n),\ldots,c_K(n)]^{\mathrm{T}}$, given by $\boldsymbol{H}_{\mathrm{eq},m}(\boldsymbol{c}(n))=\boldsymbol{H}_m+\sum_{k=1}^{K}\sqrt{\alpha}\boldsymbol{g}_k\boldsymbol{h}_{m,k}^{\mathrm{H}}c_k(n)$. Thus, Eq. (1) can also be expressed as

$$\boldsymbol{y}(l,n)=\sum_{m=1}^{M}\sqrt{P_m}\boldsymbol{H}_{\mathrm{eq},m}(\boldsymbol{c}(n))\boldsymbol{F}_m\boldsymbol{s}_m(l,n)+\boldsymbol{u}(l,n),\quad l=1,\ldots,L. \tag{2}$$

It is worth mentioning that Eq. (2) is inherently a block fading MAC channel, in which the MIMO channel matrices $\boldsymbol{H}_{\mathrm{eq},m}(\boldsymbol{c}(n))$ remain constant for every block n of L primary symbol durations, while differs in different blocks depending on the composite BD symbols $\boldsymbol{c}(n)$.

Assume that the AP knows the channel state information (CSI) for the equivalent MIMO channel $\boldsymbol{H}_{\mathrm{eq},m}(\boldsymbol{c}(n))$, say by channel training [31], while the M PTs only has the information of $\boldsymbol{H}_m$, $\boldsymbol{h}_{m,k}$ and $\boldsymbol{g}_k$, but not $\boldsymbol{H}_{\mathrm{eq},m}(\boldsymbol{c}(n))$ since they do not know the BD symbols $\boldsymbol{c}(n)$. As such, an MMSE-SIC receiver can obtain the maximum communication sum rate regardless of the decoding order of $\boldsymbol{s}_m(l,n)$ for different PTs [32]. Without loss of optimality, assume that the M PTs are decoded in order of the corresponding channel strength. Since $\|\boldsymbol{H}_{\mathrm{eq},m}(\boldsymbol{c}(n))\|^2, m=1,\ldots,M$ are random variables (r.v.) with regards to $\boldsymbol{c}(n)$, it is difficult to compare them for all PTs. Therefore, we use the asymptotic value of $\|\boldsymbol{H}_{\mathrm{eq},m}(\boldsymbol{c}(n))\|^2$ as an alternative. Specifically, for SR with large-scale BDs, i.e., $K\gg 1$, $\|\boldsymbol{H}_{\mathrm{eq},m}(\boldsymbol{c}(n))\|^2$ approaches to $\|\boldsymbol{H}_{\mathrm{eq},m}(\boldsymbol{c}(n))\|^2=\|\boldsymbol{H}_m+\sum_{k=1}^{K}\sqrt{\alpha}\boldsymbol{g}_k\boldsymbol{h}_{m,k}^{\mathrm{H}}c_k(n)\|^2\to\|\boldsymbol{H}_m+K\sqrt{\alpha}\mathbb{E}[\boldsymbol{g}_k\boldsymbol{h}_{m,k}^{\mathrm{H}}c_k(n)]\|^2=\|\boldsymbol{H}_m\|^2$. By comparing the channel strength of the direct-link MIMO channels, the decoding order can be determined. Assuming that $P_1\|\boldsymbol{H}_1\|_F^2\geqslant P_2\|\boldsymbol{H}_2\|_F^2\geqslant\ldots\geqslant P_M\|\boldsymbol{H}_M\|_F^2$ without loss of generality, then the decoding order with SIC is $1,2,\ldots,M$. When decoding PT m, the signals of PTs $1,\ldots,m-1$ have been decoded

and fully removed, while those of PTs $m+1,\ldots,M$ are considered as interference. Let $\boldsymbol{W}_m \in \mathbb{C}^{N_r \times N_m}$ denote the receive beamforming matrix for PT m. Thus, the resulting signal is written as

$$\begin{aligned}\boldsymbol{y}_m(l,n) = &\sqrt{P_m}\boldsymbol{W}_m^{\mathrm{H}}\boldsymbol{H}_{\mathrm{eq},m}(\boldsymbol{c}(n))\boldsymbol{F}_m\boldsymbol{s}_m(l,n)\\ &+\sum_{i=m+1}^{M}\sqrt{P_i}\boldsymbol{W}_m^{\mathrm{H}}\boldsymbol{H}_{\mathrm{eq},i}(\boldsymbol{c}(n))\boldsymbol{F}_i\boldsymbol{s}_i(l,n)+\boldsymbol{W}_m^{\mathrm{H}}\boldsymbol{u}(l,n).\end{aligned} \tag{3}$$

The optimal MMSE receive beamforming is

$$\boldsymbol{W}_m = \left(\sum_{i=m+1}^{M} P_i\boldsymbol{H}_{\mathrm{eq},i}(\boldsymbol{c}(n))\boldsymbol{F}_i\boldsymbol{F}_i^{\mathrm{H}}\boldsymbol{H}_{\mathrm{eq},i}^{\mathrm{H}}(\boldsymbol{c}(n))+\sigma^2\boldsymbol{I}_{N_r}\right)^{-1}\sqrt{P_m}\boldsymbol{H}_{\mathrm{eq},m}(\boldsymbol{c}(n))\boldsymbol{F}_m. \tag{4}$$

The resulting ergodic primary communication rate of PT m is

$$R_{\mathrm{PT},m} = \mathbb{E}_{\boldsymbol{c}(n)}\left[\log_2\left|\boldsymbol{I}_{N_r}+\bar{P}_m\boldsymbol{H}_{\mathrm{eq},m}\left(\boldsymbol{c}(n)\right)\boldsymbol{F}_m\boldsymbol{F}_m^{\mathrm{H}}\boldsymbol{H}_{\mathrm{eq},m}^{\mathrm{H}}(\boldsymbol{c}(n))\boldsymbol{C}_m^{-1}\right|\right], \tag{5}$$

in which $\boldsymbol{C}_m = \boldsymbol{I}_{N_r}+\sum_{i=m+1}^{M}\bar{P}_i\boldsymbol{H}_{\mathrm{eq},i}(\boldsymbol{c}(n))\boldsymbol{F}_i\boldsymbol{F}_i^{\mathrm{H}}\boldsymbol{H}_{\mathrm{eq},i}^{\mathrm{H}}(\boldsymbol{c}(n))$, and $\bar{P}_m \triangleq \frac{P_m}{\sigma^2}$ is defined as the transmit signal-to-noise ratio (SNR) of PT m. Then the sum rate of the M PTs is

$$R_{\mathrm{PT}} = \sum_{m=1}^{M} R_{\mathrm{PT},m}. \tag{6}$$

Theorem 1. The sum rate of the PTs in (6) is represented in an equivalent form as

$$R_{\mathrm{PT}} = \mathbb{E}_{\boldsymbol{c}(n)}\left[\log_2\left|\boldsymbol{I}_{N_r}+\sum_{m=1}^{M}\bar{P}_m\boldsymbol{H}_{\mathrm{eq},m}(\boldsymbol{c}(n))\boldsymbol{F}_m\boldsymbol{F}_m^{\mathrm{H}}\boldsymbol{H}_{\mathrm{eq},m}^{\mathrm{H}}(\boldsymbol{c}(n))\right|\right]. \tag{7}$$

Proof. The proofs are omitted for brevity.

Furthermore, for the AP to decode the secondary symbols $c_k(n), k=1,2,\ldots,K$, we concatenate $\boldsymbol{y}(l,n)$ in (1) for $l=1,2,\ldots,L$ to get $\boldsymbol{Y}(n)=[\boldsymbol{y}(1,n),\boldsymbol{y}(2,n),\ldots,\boldsymbol{y}(L,n)]\in\mathbb{C}^{N_r\times L}$. Using the same way, we get $\boldsymbol{S}_m(n)=[\boldsymbol{s}_m(1,n),\boldsymbol{s}_m(2,n),\ldots,\boldsymbol{s}_m(L,n)]\in\mathbb{C}^{N_m\times L}$ and $\boldsymbol{U}(n)=[\boldsymbol{u}(1,n),\boldsymbol{u}(2,n),\ldots,\boldsymbol{u}(L,n)]\in\mathbb{C}^{N_r\times L}$. Thus, Eq. (1) is rewritten as

$$\boldsymbol{Y}(n)=\sum_{m=1}^{M}\sqrt{P_m}\boldsymbol{H}_m\boldsymbol{F}_m\boldsymbol{S}_m(n)+\sum_{m=1}^{M}\sum_{k=1}^{K}\sqrt{P_m}\sqrt{\alpha}\boldsymbol{g}_k\boldsymbol{h}_{m,k}^{\mathrm{H}}\boldsymbol{F}_m\boldsymbol{S}_m(n)c_k(n)+\boldsymbol{U}(n). \tag{8}$$

When the primary signals $\boldsymbol{s}_m(l,n)$ have been decoded at the AP for all PTs and for $l=1,\ldots,L$, the first term of (8) can be removed before decoding the signals of BDs, which results in

$$\hat{\boldsymbol{Y}}(n)=\sum_{k=1}^{K}\sum_{m=1}^{M}\sqrt{P_m}\sqrt{\alpha}\boldsymbol{g}_k\boldsymbol{h}_{m,k}^{\mathrm{H}}\boldsymbol{F}_m\boldsymbol{S}_m(n)c_k(n)+\boldsymbol{U}(n). \tag{9}$$

Then we define

$$\boldsymbol{X}_k=\left[\sqrt{P_1}\boldsymbol{g}_k\boldsymbol{h}_{1,k}^{\mathrm{H}}\boldsymbol{F}_1,\ldots,\sqrt{P_M}\boldsymbol{g}_k\boldsymbol{h}_{M,k}^{\mathrm{H}}\boldsymbol{F}_M\right]\in\mathbb{C}^{N_r\times N_{\mathrm{sum}}} \tag{10}$$

and

$$\boldsymbol{S}(n)=\left[\boldsymbol{S}_1^{\mathrm{T}}(n),\ldots,\boldsymbol{S}_M^{\mathrm{T}}(n)\right]^{\mathrm{T}}\in\mathbb{C}^{N_{\mathrm{sum}}\times L}, \tag{11}$$

where $N_{\mathrm{sum}}=\sum_{m=1}^{M}N_m$ denotes the total number of data streams of the M PTs. Eq. (9) can be equivalently represented as

$$\hat{\boldsymbol{Y}}(n)=\sqrt{\alpha}\sum_{k=1}^{K}\boldsymbol{X}_k\boldsymbol{S}(n)c_k(n)+\boldsymbol{U}(n). \tag{12}$$

After decoding $\boldsymbol{S}(n)$, we can apply the temporal-domain matched filtering at the AP by right multiplying $\hat{\boldsymbol{Y}}(n)$ in (12) with $(1/\sqrt{L})\boldsymbol{S}^{\mathrm{H}}(n)$. When L is large enough, based on the fact that the information-bearing symbols $\boldsymbol{s}_m(l,n)$ are i.i.d. following distribution $\boldsymbol{s}_m(l,n)\sim\mathcal{CN}(\boldsymbol{0},\boldsymbol{I}_{N_m})$ and the law of large

numbers, there is $(1/L)\boldsymbol{S}_m(n)\boldsymbol{S}_m^{\mathrm{H}}(n) \to \boldsymbol{I}_{N_m}$, and $(1/L)\boldsymbol{S}_m(n)\boldsymbol{S}_i^{\mathrm{H}}(n) \to \boldsymbol{O}_{N_m\times N_i}, m \neq i$. Therefore, $(1/L)\boldsymbol{S}(n)\boldsymbol{S}^{\mathrm{H}}(n) \to \boldsymbol{I}_{N_{\mathrm{sum}}}$ and the resulting signal of (12) after matched filtering approaches to

$$\tilde{\boldsymbol{Y}}(n) = \frac{1}{\sqrt{L}}\hat{\boldsymbol{Y}}(n)\boldsymbol{S}^{\mathrm{H}}(n) = \sqrt{L\alpha}\sum_{k=1}^{K}\boldsymbol{X}_k c_k(n) + \tilde{\boldsymbol{U}}(n), \tag{13}$$

where $\tilde{\boldsymbol{U}}(n) = (1/\sqrt{L})\boldsymbol{U}(n)\boldsymbol{S}^{\mathrm{H}}(n) = [\tilde{\boldsymbol{u}}_1(n), \ldots, \tilde{\boldsymbol{u}}_{N_{\mathrm{sum}}}(n)] \in \mathbb{C}^{N_r\times N_{\mathrm{sum}}}$, and it can be demonstrated that $\tilde{\boldsymbol{u}}_i(n), i = 1, \ldots, N_{\mathrm{sum}}$, are i.i.d. following distribution $\mathcal{CN}\left(\boldsymbol{0}, \sigma^2\boldsymbol{I}_{N_r}\right)$. Let $\boldsymbol{y}(n) = \mathrm{vec}(\tilde{\boldsymbol{Y}}(n))$, $\boldsymbol{x}_k = \mathrm{vec}\left(\boldsymbol{X}_k\right)$, and $\boldsymbol{u}(n) = \mathrm{vec}(\tilde{\boldsymbol{U}}(n))$. Then, Eq. (13) can be equivalently expressed as

$$\boldsymbol{y}(n) = \sqrt{L\alpha}\sum_{k=1}^{K}\boldsymbol{x}_k c_k(n) + \boldsymbol{u}(n), \tag{14}$$

where $\boldsymbol{u}(n) \sim \mathcal{CN}(\boldsymbol{0}, \sigma^2\boldsymbol{I}_{N_rN_{\mathrm{sum}}})$. Note that Eq. (14) corresponds to an SIMO MAC with K users. As discussed in [30, page 424], the MMSE-SIC receiver can achieve capacity regardless of the decoding order. The sum capacity of the BDs can be accordingly written as [30, Eq. (8.71)]. Define $\boldsymbol{q}_k = \mathrm{vec}([\sqrt{P_1}\boldsymbol{g}_k\boldsymbol{h}_{1,k}^{\mathrm{H}}, \ldots, \sqrt{P_M}\boldsymbol{g}_k\boldsymbol{h}_{M,k}^{\mathrm{H}}]) \in \mathbb{C}^{N_r\times N_tM}$. The K BDs are ranked depending on their channel strength $\|\boldsymbol{q}_k\|^2$, on the basis of which the decoding order of SIC can be identified. We assume that $\|\boldsymbol{q}_1\|^2 \geqslant \|\boldsymbol{q}_2\|^2 \geqslant \cdots \geqslant \|\boldsymbol{q}_K\|^2$ without loss of generality. Then the decoding order with SIC is $1, 2, \ldots, K$. Take decoding BD k as an example, when the AP has decoded and fully subtracted the signals of BDs $1, \ldots, k-1$, while it treats the signals of BDs $k+1, \ldots, K$ as interference. Let $\boldsymbol{w}_k \in \mathbb{C}^{N_rN_{\mathrm{sum}}\times 1}$ represent the beamforming vector of BD k. Thus, the resulting signal is

$$y_k(n) = \sqrt{L\alpha}\boldsymbol{w}_k^{\mathrm{H}}\boldsymbol{x}_k c_k(n) + \sqrt{L\alpha}\boldsymbol{w}_k^{\mathrm{H}}\sum_{i=k+1}^{K}\boldsymbol{x}_i c_i(n) + \boldsymbol{w}_k^{\mathrm{H}}\boldsymbol{u}(n). \tag{15}$$

The resulting SINR for BD k is

$$\gamma_{\mathrm{BD},k} = \frac{L\alpha\left|\boldsymbol{w}_k^{\mathrm{H}}\boldsymbol{x}_k\right|^2}{L\alpha\sum_{i=k+1}^{K}\left|\boldsymbol{w}_k^{\mathrm{H}}\boldsymbol{x}_i\right|^2 + \sigma^2\|\boldsymbol{w}_k\|^2}. \tag{16}$$

The SINR-maximizing MMSE beamforming can be written as

$$\boldsymbol{w}_k = \left(\sum_{i=k+1}^{K}L\alpha\boldsymbol{x}_i\boldsymbol{x}_i^{\mathrm{H}} + \sigma^2\boldsymbol{I}_{N_rN_{\mathrm{sum}}}\right)^{-1}\sqrt{L\alpha}\boldsymbol{x}_k. \tag{17}$$

The corresponding SINR is thus derived as

$$\gamma_{\mathrm{BD},k} = L\alpha\boldsymbol{x}_k^{\mathrm{H}}\left(\sum_{i=k+1}^{K}L\alpha\boldsymbol{x}_i\boldsymbol{x}_i^{\mathrm{H}} + \sigma^2\boldsymbol{I}_{N_rN_{\mathrm{sum}}}\right)^{-1}\boldsymbol{x}_k. \tag{18}$$

Then the sum rate of the K BDs is

$$R_{\mathrm{BD}} = \frac{1}{L}\sum_{k=1}^{K}\log_2\left(1 + \gamma_{\mathrm{BD},k}\right), \tag{19}$$

in which the pre-log factor $1/L$ suggests that in our considered setup of CSR, the symbol rate of the active PTs is L times that of the passive BDs.

By using the similar derivations as Appendix A of [28], the sum rate in (19) is also expressed as

$$R_{\mathrm{BD}} = \frac{1}{L}\log_2\left|\boldsymbol{I}_{N_rN_{\mathrm{sum}}} + \frac{L\alpha}{\sigma^2}\sum_{k=1}^{K}\boldsymbol{x}_k\boldsymbol{x}_k^{\mathrm{H}}\right|, \tag{20}$$

in which the pre-log factor $1/L$ suggests that the symbol duration of the BDs is L times that of the PTs, which, however, results in the processing gain indicated by the factor L inside the determinant.

3.2 Asymptotic rate analysis

In this subsection, we study the asymptotic performance of SR including multiple PTs and massive BDs, i.e., the number of BDs K goes to sufficiently large. To achieve tractable asymptotic performance evaluation, we assume that for all the K BDs, the channels $\boldsymbol{h}_{m,k}$ and $\boldsymbol{g}_k$ are i.i.d. distributed with zero mean, and $\mathbb{E}[\boldsymbol{h}_{m,k}\boldsymbol{h}_{m,k}^{\mathrm{H}}] = \beta_{h,m}\boldsymbol{I}_{N_t}$, $\mathbb{E}[\boldsymbol{g}_k\boldsymbol{g}_k^{\mathrm{H}}] = \beta_g\boldsymbol{I}_{N_r}$, $k = 1, \ldots, K$, with $\beta_{h,m}$ and β_g being the large-scale channel gains. Assume that the entries of $\boldsymbol{H}_m, m = 1, \ldots, M$ are i.i.d. CSCG random variables with mean zero and variance $\beta_{\mathrm{H},m}, m = 1, \ldots, M$, respectively. First, the asymptotic behavior of the sum rate of the BDs is analyzed as follows.

Lemma 1. For SR with large-scale BDs, i.e., $K \gg 1$, the sum rate of K BDs in (20) approaches to

$$R_{\mathrm{BD}} \to \frac{N_r}{L}\sum_{m=1}^{M}\log_2\left|\boldsymbol{I}_{N_t} + KL\bar{P}_m\alpha\beta_{h,m}\beta_g\boldsymbol{F}_m\boldsymbol{F}_m^{\mathrm{H}}\right|. \tag{21}$$

Proof. Please see Appendix A.

Note that Lemma 1 provides a more generic result considering multiuser SR systems than our previous work [28], which only considered a single PT case. It is shown in Lemma 1 that R_{BD} increases with the number of BDs K, as the result of the multi-user diversity gains. In addition, compared with the single PT case studied in [28], multiple PTs can provide enhanced ambient RF signals, so that R_{BD} also increases with the number of PTs M.

If the design objective is to find the transmit precoding matrices $\{\boldsymbol{F}_m\}_{m=1}^M$ to maximize the asymptotic rate of BDs regardless of that of the PTs, then we can formulate the optimization problem based on Lemma 1 as

$$\max_{\substack{\boldsymbol{F}_m, N_m \leqslant N_t,\\ m=1,\ldots,M}} \frac{N_r}{L}\sum_{m=1}^{M}\log_2\left|\boldsymbol{I}_{N_t} + KL\bar{P}_m\alpha\beta_g\beta_{h,m}\boldsymbol{F}_m\boldsymbol{F}_m^{\mathrm{H}}\right| \tag{22a}$$

$$\text{s.t.} \quad \mathrm{tr}\left(\boldsymbol{F}_m\boldsymbol{F}_m^{\mathrm{H}}\right) \leqslant 1, \ \forall m. \tag{22b}$$

By following similar derivations as [28], the optimal solution can be obtained when $\boldsymbol{F}_m\boldsymbol{F}_m^{\mathrm{H}} = \frac{1}{N_t}\boldsymbol{I}_{N_t}, m = 1, \ldots, M$, and the optimal objective value is

$$R_{\mathrm{BD}} \to R_{\mathrm{BD}}^{\mathrm{asym}} = \frac{N_r N_t}{L}\sum_{m=1}^{M}\log_2\left(1 + \frac{KL\bar{P}_m\alpha\beta_g\beta_{h,m}}{N_t}\right). \tag{23}$$

Accordingly, since $\mathrm{rank}\,(\boldsymbol{F}_m) = N_t, m = 1, \ldots, M$, the optimal number of data streams N_m for each PT is N_t.

Lemma 2. For multiuser MIMO SR with massive BDs and massive receive antennas, i.e., $K \gg 1$ and $N_r \gg 1$, the sum rate of the M PTs in (7) approaches to

$$R_{\mathrm{PT}} \to \sum_{m=1}^{M}\log_2\left|\boldsymbol{I}_{N_t} + \bar{P}_m N_r\left(\beta_{\mathrm{H},m} + K\alpha\beta_g\beta_{h,m}\right)\boldsymbol{F}_m\boldsymbol{F}_m^{\mathrm{H}}\right|. \tag{24}$$

Proof. Please see Appendix B.

According to Lemma 2, the asymptotic sum rate of PTs R_{PT} also increases with the number of PTs M and BDs K, since multiple PTs provide multi-user diversity gain and massive BDs create multi-path gain to the primary communication link of each PT.

If the design objective is to find the transmit precoding matrices $\{\boldsymbol{F}_m\}_{m=1}^M$ to maximize the asymptotic rate of PTs regardless of that of the BDs, then the optimization problem based on Lemma 2 is

$$\max_{\substack{\boldsymbol{F}_m, N_m \leqslant N_t,\\ m=1,\ldots,M}} \sum_{m=1}^{M}\log_2\left|\boldsymbol{I}_{N_t} + \bar{P}_m N_r\left(\beta_{\mathrm{H},m} + K\alpha\beta_g\beta_{h,m}\right)\boldsymbol{F}_m\boldsymbol{F}_m^{\mathrm{H}}\right| \tag{25a}$$

$$\text{s.t.} \quad \mathrm{tr}\left(\boldsymbol{F}_m\boldsymbol{F}_m^{\mathrm{H}}\right) \leqslant 1, \forall m. \tag{25b}$$

Similar to problem (22), the optimal solution to problem (25) can be obtained when $\boldsymbol{F}_m\boldsymbol{F}_m^{\mathrm{H}} = \frac{1}{N_t}\boldsymbol{I}_{N_t}, m = 1,\ldots,M$ and $N_m = N_t$. That is to say, when the number of BDs K goes to sufficiently large, there is a win-win situation for both the primary and the secondary communication with proper precoding. This thus demonstrates that massive BD access can fully enable the mutualism relationship of SR. By substituting the optimal solution $\boldsymbol{F}_m\boldsymbol{F}_m^{\mathrm{H}} = \frac{1}{N_t}\boldsymbol{I}_{N_t}, m = 1,\ldots,M$, the optimal asymptotic sum rate of primary communication is

$$\begin{aligned} R_{\mathrm{PT}} &\to R_{\mathrm{PT}}^{\mathrm{asym}} \\ &= \sum_{m=1}^{M} \log_2 \left| \left(1 + \frac{\bar{P}_m N_r}{N_t}\left(\beta_{\mathrm{H},m} + K\alpha\beta_g\beta_{h,m}\right)\right)\boldsymbol{I}_{N_t} \right| \\ &= N_t \sum_{m=1}^{M} \log_2 \left(1 + \frac{\bar{P}_m N_r}{N_t}\left(\beta_{\mathrm{H},m} + K\alpha\beta_g\beta_{h,m}\right)\right). \end{aligned} \tag{26}$$

4 Precoding optimization

In this section, for practical systems with a certain finite number of BDs K, we study the precoding optimization problem, with the objective to maximize the sum rate of PTs in (7), while satisfying the sum rate constraint of BDs in (20). In addition, we also consider the minimum communication rate constraint for the PTs and BDs in the prescribed active and passive user subsets, which may correspond to users with high communication priorities. Specifically, let $\mathcal{P} \subset \{1,\ldots,M\}$ denote the subset of the M PTs, for which a minimum active communication rate requirement r_s should be guaranteed. Similarly, let $\mathcal{B} \subset \{1,\ldots,K\}$ denote the subset of the K BDs that have a minimum passive communication rate requirement r_c. Then we can formulate the transmit precoding optimization problem as

$$\max_{\substack{\boldsymbol{F}_m\in\mathbb{C}^{N_t\times N_m},\\ N_m\leqslant N_t,\\ m=1,\ldots,M}} \mathbb{E}_{\boldsymbol{c}(n)}\left[\log_2\left|\boldsymbol{I}_{N_r} + \sum_{m=1}^{M}\bar{P}_m\boldsymbol{H}_{\mathrm{eq},m}(\boldsymbol{c}(n))\boldsymbol{F}_m\boldsymbol{F}_m^{\mathrm{H}}\boldsymbol{H}_{\mathrm{eq},m}^{\mathrm{H}}(\boldsymbol{c}(n))\right|\right] \tag{27a}$$

$$\text{s.t.} \quad \frac{1}{L}\log_2\left|\boldsymbol{I}_{N_rN_{\mathrm{sum}}} + \frac{L\alpha}{\sigma^2}\sum_{k=1}^{K}\boldsymbol{x}_k\boldsymbol{x}_k^{\mathrm{H}}\right| \geqslant r_{\mathrm{BD}}, \tag{27b}$$

$$\mathbb{E}_{\boldsymbol{c}(n)}\left[\log_2\left|\boldsymbol{I}_{N_r} + \bar{P}_m\boldsymbol{H}_{\mathrm{eq},m}(\boldsymbol{c}(n))\boldsymbol{F}_m\boldsymbol{F}_m^{\mathrm{H}}\boldsymbol{H}_{\mathrm{eq},m}^{\mathrm{H}}(\boldsymbol{c}(n))\boldsymbol{C}_m^{-1}\right|\right] \geqslant r_s,\ \forall m\in\mathcal{P}, \tag{27c}$$

$$\frac{1}{L}\log_2\left(1 + L\alpha\boldsymbol{x}_k^{\mathrm{H}}\left(\sum_{i=k+1}^{K}L\alpha\boldsymbol{x}_i\boldsymbol{x}_i^{\mathrm{H}} + \sigma^2\boldsymbol{I}_{N_rN_{\mathrm{sum}}}\right)^{-1}\boldsymbol{x}_k\right) \geqslant r_c,\ \forall k\in\mathcal{B}, \tag{27d}$$

$$\mathrm{tr}\big(\boldsymbol{F}_m\boldsymbol{F}_m^{\mathrm{H}}\big) \leqslant 1,\ \forall m, \tag{27e}$$

where

$$\boldsymbol{x}_k = \mathrm{vec}\big[\sqrt{P_1}\boldsymbol{g}_k\boldsymbol{h}_{1,k}^{\mathrm{H}}\boldsymbol{F}_1,\ldots,\sqrt{P_M}\boldsymbol{g}_k\boldsymbol{h}_{M,k}^{\mathrm{H}}\boldsymbol{F}_M\big], \tag{28}$$

for $k = 1,\ldots,K$, are variables consisting of $\boldsymbol{F}_m$, $m = 1,\ldots,M$. r_{BD} denotes the minimum threshold for the sum rate of the K BDs. Notice that the optimization variables in problem (27) include not only the precoding matrices $\boldsymbol{F}_m \in \mathbb{C}^{N_t\times N_m}$, but also the number of data streams N_m. However, directly optimizing $\boldsymbol{F}_m$ and N_m is difficult. Fortunately, it has been demonstrated that if the optimal transmit covariance matrices $\boldsymbol{Q}_m \triangleq (\boldsymbol{F}_m\boldsymbol{F}_m^{\mathrm{H}})$ are determined, then the optimal $\boldsymbol{F}_m$ and N_m can be obtained accordingly [28]. To this end, we need to find the equivalent rate expressions in the objective cost functions with regard to the transmit covariance matrices $\boldsymbol{Q}_m$, as pursued in the following. According to (5), the left hand side

of (27c) is also expressed as

$$\begin{aligned} R_{\mathrm{PT},m} &= \mathbb{E}_{\boldsymbol{c}(n)}\left[\log_2\left|\boldsymbol{I}_{N_r}+\bar{P}_m\boldsymbol{H}_{\mathrm{eq},m}(\boldsymbol{c}(n))\boldsymbol{F}_m\boldsymbol{F}_m^{\mathrm{H}}\boldsymbol{H}_{\mathrm{eq},m}^{\mathrm{H}}(\boldsymbol{c}(n))\boldsymbol{C}_m^{-1}\right|\right] \\ &= \mathbb{E}_{\boldsymbol{c}(n)}\left[\log_2\left|\boldsymbol{I}_{N_r}+\sum_{i=m}^{M}\bar{P}_i\boldsymbol{H}_{\mathrm{eq},i}(\boldsymbol{c}(n))\boldsymbol{F}_i\boldsymbol{F}_i^{\mathrm{H}}\boldsymbol{H}_{\mathrm{eq},i}^{\mathrm{H}}(\boldsymbol{c}(n))\right|\right] \\ &\quad - \mathbb{E}_{\boldsymbol{c}(n)}\left[\log_2\left|\boldsymbol{I}_{N_r}+\sum_{i=m+1}^{M}\bar{P}_i\boldsymbol{H}_{\mathrm{eq},i}(\boldsymbol{c}(n))\boldsymbol{F}_i\boldsymbol{F}_i^{\mathrm{H}}\boldsymbol{H}_{\mathrm{eq},i}^{\mathrm{H}}(\boldsymbol{c}(n))\right|\right], \end{aligned} \tag{29}$$

in which the last equality holds for the identity $|\boldsymbol{X}\boldsymbol{Y}| = |\boldsymbol{X}| \times |\boldsymbol{Y}|$.

Furthermore, define $\boldsymbol{G} = [\boldsymbol{x}_1, \boldsymbol{x}_2, \ldots, \boldsymbol{x}_K] \in \mathbb{C}^{N_r N_{\mathrm{sum}} \times K}$. The left hand side of (27b) is expressed as

$$\begin{aligned} R_{\mathrm{BD}} &= \frac{1}{L}\log_2\left|\boldsymbol{I}_{N_r N_{\mathrm{sum}}}+\frac{L\alpha}{\sigma^2}\sum_{k=1}^{K}\boldsymbol{x}_k\boldsymbol{x}_k^{\mathrm{H}}\right| \\ &= \frac{1}{L}\log_2\left|\boldsymbol{I}_{N_r N_{\mathrm{sum}}}+\frac{L\alpha}{\sigma^2}\boldsymbol{G}\boldsymbol{G}^{\mathrm{H}}\right| \\ &= \frac{1}{L}\log_2\left|\boldsymbol{I}_K+\frac{L\alpha}{\sigma^2}\boldsymbol{G}^{\mathrm{H}}\boldsymbol{G}\right|, \end{aligned} \tag{30}$$

where the last equality holds due to the Weinstein-Aronszajn identity $|\boldsymbol{I}_m + \boldsymbol{X}\boldsymbol{Y}| = |\boldsymbol{I}_n + \boldsymbol{Y}\boldsymbol{X}|$. According to the identity $\mathrm{vec}(\boldsymbol{X}_1\boldsymbol{X}_2\boldsymbol{X}_3) = \left(\boldsymbol{X}_3^{\mathrm{T}} \otimes \boldsymbol{X}_1\right)\mathrm{vec}(\boldsymbol{X}_2)$, $\boldsymbol{x}_k$ can be written as

$$\begin{aligned} \boldsymbol{x}_k &= \left[\mathrm{vec}^{\mathrm{T}}\left(\sqrt{P_1}\boldsymbol{g}_k\boldsymbol{h}_{1,k}^{\mathrm{H}}\boldsymbol{F}_1\right), \ldots, \mathrm{vec}^{\mathrm{T}}\left(\sqrt{P_M}\boldsymbol{g}_k\boldsymbol{h}_{M,k}^{\mathrm{H}}\boldsymbol{F}_M\right)\right]^{\mathrm{T}} \\ &= \begin{bmatrix} \sqrt{P_1}\boldsymbol{F}_1^{\mathrm{T}} \otimes \left(\boldsymbol{g}_k\boldsymbol{h}_{1,k}^{\mathrm{H}}\right) \\ \vdots \\ \sqrt{P_M}\boldsymbol{F}_M^{\mathrm{T}} \otimes \left(\boldsymbol{g}_k\boldsymbol{h}_{M,k}^{\mathrm{H}}\right) \end{bmatrix} \mathrm{vec}(\boldsymbol{I}_{N_t}). \end{aligned} \tag{31}$$

For notational convenience, let

$$\boldsymbol{L}_{m,k} = \left[\boldsymbol{g}_k\boldsymbol{h}_{m,k}^{\mathrm{H}}, \ldots, \boldsymbol{g}_K\boldsymbol{h}_{m,K}^{\mathrm{H}}\right] \in \mathbb{C}^{N_r \times N_t(K-k+1)}, \tag{32}$$

and

$$\boldsymbol{\Psi}_k = \begin{bmatrix} \mathrm{vec}(\boldsymbol{I}_{N_t}) & \boldsymbol{0}_{N_t} & \ldots & \boldsymbol{0}_{N_t} \\ \boldsymbol{0}_{N_t} & \mathrm{vec}(\boldsymbol{I}_{N_t}) & \ldots & \boldsymbol{0}_{N_t} \\ \vdots & \vdots & \ddots & \vdots \\ \boldsymbol{0}_{N_t} & \boldsymbol{0}_{N_t} & \ldots & \mathrm{vec}(\boldsymbol{I}_{N_t}) \end{bmatrix} \in \mathbb{C}^{N_t^2(K-k+1)\times(K-k+1)}, \tag{33}$$

then $\boldsymbol{G}$ is expressed as

$$\begin{aligned} \boldsymbol{G} &= \begin{bmatrix} \sqrt{P_1}\boldsymbol{F}_1^{\mathrm{T}} \otimes \boldsymbol{g}_1\boldsymbol{h}_{1,1}^{\mathrm{H}} & \sqrt{P_1}\boldsymbol{F}_1^{\mathrm{T}} \otimes \boldsymbol{g}_2\boldsymbol{h}_{1,2}^{\mathrm{H}} & \ldots & \sqrt{P_1}\boldsymbol{F}_1^{\mathrm{T}} \otimes \boldsymbol{g}_K\boldsymbol{h}_{1,K}^{\mathrm{H}} \\ \vdots & \vdots & \ddots & \vdots \\ \sqrt{P_M}\boldsymbol{F}_M^{\mathrm{T}} \otimes \boldsymbol{g}_1\boldsymbol{h}_{M,1}^{\mathrm{H}} & \sqrt{P_M}\boldsymbol{F}_M^{\mathrm{T}} \otimes \boldsymbol{g}_2\boldsymbol{h}_{M,2}^{\mathrm{H}} & \ldots & \sqrt{P_M}\boldsymbol{F}_M^{\mathrm{T}} \otimes \boldsymbol{g}_J\boldsymbol{h}_{M,J}^{\mathrm{H}} \end{bmatrix} \begin{bmatrix} \mathrm{vec}(\boldsymbol{I}_{N_t}) & \boldsymbol{0}_{N_t} & \ldots & \boldsymbol{0}_{N_t} \\ \boldsymbol{0}_{N_t} & \mathrm{vec}(\boldsymbol{I}_{N_t}) & \ldots & \boldsymbol{0}_{N_t} \\ \vdots & \vdots & \ddots & \vdots \\ \boldsymbol{0}_{N_t} & \boldsymbol{0}_{N_t} & \ldots & \mathrm{vec}(\boldsymbol{I}_{N_t}) \end{bmatrix} \\ &= \begin{bmatrix} \sqrt{P_1}\boldsymbol{F}_1^{\mathrm{T}} \otimes \left[\boldsymbol{g}_1\boldsymbol{h}_{1,1}^{\mathrm{H}}, \boldsymbol{g}_2\boldsymbol{h}_{1,2}^{\mathrm{H}}, \ldots, \boldsymbol{g}_K\boldsymbol{h}_{1,K}^{\mathrm{H}}\right] \\ \vdots \\ \sqrt{P_M}\boldsymbol{F}_M^{\mathrm{T}} \otimes \left[\boldsymbol{g}_1\boldsymbol{h}_{M,1}^{\mathrm{H}}, \boldsymbol{g}_2\boldsymbol{h}_{M,2}^{\mathrm{H}}, \ldots, \boldsymbol{g}_K\boldsymbol{h}_{M,K}^{\mathrm{H}}\right] \end{bmatrix} \begin{bmatrix} \mathrm{vec}(\boldsymbol{I}_{N_t}) & \boldsymbol{0}_{N_t} & \ldots & \boldsymbol{0}_{N_t} \\ \boldsymbol{0}_{N_t} & \mathrm{vec}(\boldsymbol{I}_{N_t}) & \ldots & \boldsymbol{0}_{N_t} \\ \vdots & \vdots & \ddots & \vdots \\ \boldsymbol{0}_{N_t} & \boldsymbol{0}_{N_t} & \ldots & \mathrm{vec}(\boldsymbol{I}_{N_t}) \end{bmatrix} \\ &= \begin{bmatrix} \sqrt{P_1}\boldsymbol{F}_1^{\mathrm{T}} \otimes \boldsymbol{L}_{1,1} \\ \vdots \\ \sqrt{P_M}\boldsymbol{F}_M^{\mathrm{T}} \otimes \boldsymbol{L}_{M,1} \end{bmatrix} \boldsymbol{\Psi}_1. \end{aligned} \tag{34}$$

According to (30), R_{BD} can also be expressed as

$$\begin{aligned} R_{\mathrm{BD}} &= \frac{1}{L}\log_2\left|\boldsymbol{I}_K+\frac{L\alpha}{\sigma^2}\boldsymbol{G}^{\mathrm{T}}\boldsymbol{G}^*\right| \\ &= \frac{1}{L}\log_2\left|\boldsymbol{I}_K+\frac{L\alpha}{\sigma^2}\boldsymbol{\Psi}_1^{\mathrm{T}}\left(\sum_{m=1}^{M}P_m\left(\boldsymbol{F}_m^{\mathrm{T}}\otimes\boldsymbol{L}_{m,1}\right)^{\mathrm{T}}\left(\boldsymbol{F}_m^{\mathrm{T}}\otimes\boldsymbol{L}_{m,1}\right)^*\right)\boldsymbol{\Psi}_1^*\right| \\ &= \frac{1}{L}\log_2\left|\boldsymbol{I}_K+L\alpha\boldsymbol{\Psi}_1^{\mathrm{H}}\left(\sum_{m=1}^{M}\bar{P}_m\left(\boldsymbol{F}_m\boldsymbol{F}_m^{\mathrm{H}}\right)\otimes\left(\boldsymbol{L}_{m,1}^{\mathrm{H}}\boldsymbol{L}_{m,1}\right)^{\mathrm{T}}\right)\boldsymbol{\Psi}_1\right|, \end{aligned} \tag{35}$$

in which the first equality holds for the identity $|\boldsymbol{X}|=\left|\boldsymbol{X}^{\mathrm{T}}\right|$, the last equality holds for the fact that $(\boldsymbol{X}\otimes\boldsymbol{Y})^{\mathrm{T}}=\boldsymbol{X}^{\mathrm{T}}\otimes\boldsymbol{Y}^{\mathrm{T}}$, $(\boldsymbol{X}\otimes\boldsymbol{Y})^*=\boldsymbol{X}^*\otimes\boldsymbol{Y}^*$, $(\boldsymbol{X}_1\otimes\boldsymbol{X}_2)(\boldsymbol{X}_3\otimes\boldsymbol{X}_4)=(\boldsymbol{X}_1\boldsymbol{X}_3)\otimes(\boldsymbol{X}_2\boldsymbol{X}_4)$ and $\boldsymbol{\Psi}_1\in\mathbb{R}$.

Furthermore, the communication rate of BD k on the left hand side of (27d) is also expressed as

$$\begin{aligned} R_{\mathrm{BD},k} &= \frac{1}{L}\log_2\left(1+L\alpha\boldsymbol{x}_k^{\mathrm{H}}\left(\sum_{i=k+1}^{K}L\alpha\boldsymbol{x}_i\boldsymbol{x}_i^{\mathrm{H}}+\sigma^2\boldsymbol{I}_{N_rN_{\mathrm{sum}}}\right)^{-1}\boldsymbol{x}_k\right) \\ &= \frac{1}{L}\log_2\left|\boldsymbol{I}_{N_rN_{\mathrm{sum}}}+L\alpha\boldsymbol{x}_k\boldsymbol{x}_k^{\mathrm{H}}\left(\sum_{i=k+1}^{K}L\alpha\boldsymbol{x}_i\boldsymbol{x}_i^{\mathrm{H}}+\sigma^2\boldsymbol{I}_{N_rN_{\mathrm{sum}}}\right)^{-1}\right| \\ &= \frac{1}{L}\log_2\left|\left(\sum_{i=k+1}^{K}L\alpha\boldsymbol{x}_i\boldsymbol{x}_i^{\mathrm{H}}+\sigma^2\boldsymbol{I}_{N_rN_{\mathrm{sum}}}+L\alpha\boldsymbol{x}_k\boldsymbol{x}_k^{\mathrm{H}}\right)\left(\sum_{i=k+1}^{K}L\alpha\boldsymbol{x}_i\boldsymbol{x}_i^{\mathrm{H}}+\sigma^2\boldsymbol{I}_{N_rN_{\mathrm{sum}}}\right)^{-1}\right| \\ &= \frac{1}{L}\log_2\left|\boldsymbol{I}_{N_rN_{\mathrm{sum}}}+\frac{L\alpha}{\sigma^2}\sum_{i=k}^{K}\boldsymbol{x}_i\boldsymbol{x}_i^{\mathrm{H}}\right|-\frac{1}{L}\log_2\left|\boldsymbol{I}_{N_rN_{\mathrm{sum}}}+\frac{L\alpha}{\sigma^2}\sum_{i=k+1}^{K}\boldsymbol{x}_i\boldsymbol{x}_i^{\mathrm{H}}\right|. \end{aligned} \tag{36}$$

Similar to (35), the result in (36) is expressed as

$$\begin{aligned} R_{\mathrm{BD},k} =& \frac{1}{L}\log_2\left|\boldsymbol{I}_{(K-k+1)}+L\alpha\boldsymbol{\Psi}_k^{\mathrm{H}}\left(\sum_{m=1}^{M}\bar{P}_m\left(\boldsymbol{F}_m\boldsymbol{F}_m^{\mathrm{H}}\right)\otimes\left(\boldsymbol{L}_{m,k}^{\mathrm{H}}\boldsymbol{L}_{m,k}\right)^{\mathrm{T}}\right)\boldsymbol{\Psi}_k\right| \\ &-\frac{1}{K}\log_2\left|\boldsymbol{I}_{(K-k)}+K\alpha\boldsymbol{\Psi}_{k+1}^{\mathrm{H}}\left(\sum_{m=1}^{M}\bar{P}_m\left(\boldsymbol{F}_m\boldsymbol{F}_m^{\mathrm{H}}\right)\otimes\left(\boldsymbol{L}_{m,k+1}^{\mathrm{H}}\boldsymbol{L}_{m,k+1}\right)^{\mathrm{T}}\right)\boldsymbol{\Psi}_{k+1}\right|. \end{aligned} \tag{37}$$

By substituting the left hand side of (27b)–(27d) with (29), (35), and (37), respectively, problem (27) can be equivalently expressed as

$$\max_{\substack{\boldsymbol{F}_m\in\mathbb{C}^{N_t\times N_m},\\ N_m\leqslant N_t,\\ m=1,\ldots,M}} \mathbb{E}_{\boldsymbol{c}(n)}\left[\log_2\left|\boldsymbol{I}_{N_r}+\sum_{m=1}^{M}\bar{P}_m\boldsymbol{H}_{\mathrm{eq},m}(\boldsymbol{c}(n))\boldsymbol{F}_m\boldsymbol{F}_m^{\mathrm{H}}\boldsymbol{H}_{\mathrm{eq},m}^{\mathrm{H}}(\boldsymbol{c}(n))\right|\right] \tag{38a}$$

$$\text{s.t.}\quad \frac{1}{L}\log_2\left|\boldsymbol{I}_K+L\alpha\boldsymbol{\Psi}_1^{\mathrm{H}}\left(\sum_{m=1}^{M}\bar{P}_m\left(\boldsymbol{F}_m\boldsymbol{F}_m^{\mathrm{H}}\right)\otimes\left(\boldsymbol{L}_{m,1}^{\mathrm{H}}\boldsymbol{L}_{m,1}\right)^{\mathrm{T}}\right)\boldsymbol{\Psi}_1\right|\geqslant r_{\mathrm{BD}}, \tag{38b}$$

$$R_{\mathrm{PT},m}\geqslant r_s,\ m\in\mathcal{P}, \tag{38c}$$

$$R_{\mathrm{BD},k}\geqslant r_c,\ k\in\mathcal{B}, \tag{38d}$$

$$\mathrm{tr}\left(\boldsymbol{F}_m\boldsymbol{F}_m^{\mathrm{H}}\right)\leqslant 1,\ \forall m. \tag{38e}$$

By defining the transmit covariance matrices $\boldsymbol{Q}_m\triangleq\boldsymbol{F}_m\boldsymbol{F}_m^{\mathrm{H}}, m=1,\ldots,M$, problem (38) is equivalently written as

$$\max_{\substack{\boldsymbol{Q}_m,\\ m=1,\ldots,M}} \mathbb{E}_{\boldsymbol{c}(n)}\left[\log_2\left|\boldsymbol{I}_{N_r}+\sum_{m=1}^{M}\bar{P}_m\boldsymbol{H}_{\mathrm{eq},m}(\boldsymbol{c}(n))\boldsymbol{Q}_m\boldsymbol{H}_{\mathrm{eq},m}^{\mathrm{H}}(\boldsymbol{c}(n))\right|\right] \tag{39a}$$

$$\text{s.t.} \quad \frac{1}{L}\log_2\left|\boldsymbol{I}_K + L\alpha\boldsymbol{\Psi}_1^{\mathrm{H}}\left(\sum_{m=1}^{M}\bar{P}_m\boldsymbol{Q}_m\otimes\left(\boldsymbol{L}_{m,1}^{\mathrm{H}}\boldsymbol{L}_{m,1}\right)^{\mathrm{T}}\right)\boldsymbol{\Psi}_1\right| \geqslant r_{\mathrm{BD}}, \tag{39b}$$

$$R_{\mathrm{PT},m} \geqslant r_s,\ m\in\mathcal{P}, \tag{39c}$$

$$R_{\mathrm{BD},k} \geqslant r_c,\ k\in\mathcal{B}, \tag{39d}$$

$$\mathrm{tr}\left(\boldsymbol{Q}_m\right) \leqslant 1,\ \boldsymbol{Q}_m \succeq 0,\ \forall m. \tag{39e}$$

In problem (39), the optimization variables are the transmit covariance matrices $\boldsymbol{Q}_m$. Once we have obtained the optimal transmit covariance matrices $\boldsymbol{Q}_m^{\star}$ to problem (39), by using the simple eigen-decomposition method as in [28], the corresponding optimal precoding matrices $\boldsymbol{F}_m$ and the number of data streams N_m can be obtained. Therefore, finding the solution to problem (39) is equivalent to solving problem (27).

Note that there are two challenges for solving (39). Firstly, the communication rate of the PTs involves an expectation with respect to $\boldsymbol{c}(n)$, for which no closed-form expression can be obtained in general. Secondly, problem (39) is non-convex for the non-convex constraints such as (39c) and (39d). To address the first challenges, in the following, we use the sample average of the primary communication in (39a) and (39c) to approximate the expected values. Consider S independent realizations of $\boldsymbol{c}(n)$, which are denoted as $\boldsymbol{c}_s, s=1,\ldots,S$. When S is sufficiently large, problem (39) can be written as

$$\max_{\substack{\boldsymbol{Q}_m,\\ m=1,\ldots,M}} \frac{1}{S}\sum_{s=1}^{S}\left(\log_2\left|\boldsymbol{I}_{N_r}+\sum_{m=1}^{M}\bar{P}_m\boldsymbol{H}_{\mathrm{eq},m}\left(\boldsymbol{c}_s(n)\right)\boldsymbol{Q}_m\boldsymbol{H}_{\mathrm{eq},m}^{\mathrm{H}}\left(\boldsymbol{c}_s(n)\right)\right|\right) \tag{40a}$$

$$\text{s.t.} \quad \frac{1}{L}\log_2\left|\boldsymbol{I}_K + L\alpha\boldsymbol{\Psi}_1^{\mathrm{H}}\left(\sum_{m=1}^{M}\bar{P}_m\boldsymbol{Q}_m\otimes\left(\boldsymbol{L}_{m,1}^{\mathrm{H}}\boldsymbol{L}_{m,1}\right)^{\mathrm{T}}\right)\boldsymbol{\Psi}_1\right| \geqslant r_{\mathrm{BD}}, \tag{40b}$$

$$R_{\mathrm{PT},m,\mathrm{sample}} \geqslant r_s,\ m\in\mathcal{P}, \tag{40c}$$

$$R_{\mathrm{BD},k,\mathrm{low}} \geqslant r_c,\ k\in\mathcal{B}, \tag{40d}$$

$$\mathrm{tr}\left(\boldsymbol{Q}_m\right) \leqslant 1,\ \boldsymbol{Q}_m \succeq 0,\ \forall m, \tag{40e}$$

where $R_{\mathrm{PT},m,\mathrm{sample}}$ is the sample average of $R_{\mathrm{PT},m,}$. To address the non-convex constraints (40c) and (40d), we utilize the SCA technique, which is an iterative method to transform the non-convex problem into a sequence of convex optimization subproblems [33–36]. Specifically, for the iteration l, denote the local point obtained by the previous iteration process as $\boldsymbol{Q}_m^{(l)}$. Let

$$R_{\mathrm{PT},m,\mathrm{sample}} = \frac{1}{S}\sum_{s=1}^{S}\left(\log_2\left|\boldsymbol{I}_{N_r}+\sum_{i=m}^{M}\bar{P}_i\boldsymbol{H}_{\mathrm{eq},i}\left(\boldsymbol{c}_s(n)\right)\boldsymbol{Q}_i\boldsymbol{H}_{\mathrm{eq},i}^{\mathrm{H}}\left(\boldsymbol{c}_s(n)\right)\right|\right) - y_1(\boldsymbol{Q}_{m+1},\ldots,\boldsymbol{Q}_M), \tag{41}$$

where

$$y_1(\boldsymbol{Q}_{m+1},\ldots,\boldsymbol{Q}_M) = \frac{1}{S}\sum_{s=1}^{S}\left(\log_2\left|\boldsymbol{I}_{N_r}+\sum_{i=m+1}^{M}\bar{P}_i\boldsymbol{H}_{\mathrm{eq},i}\left(\boldsymbol{c}_s(n)\right)\boldsymbol{Q}_i\boldsymbol{H}_{\mathrm{eq},i}^{\mathrm{H}}\left(\boldsymbol{c}_s(n)\right)\right|\right). \tag{42}$$

$y_1(\boldsymbol{Q}_{m+1},\ldots,\boldsymbol{Q}_M)$ is a concave differentiable function related to $\boldsymbol{Q}_i, i=m+1,\ldots,M$. According to the fact that the first-order Taylor expansion of a concave differentiable function can provide a global upper bound [37, 38], there is

$$\begin{aligned} &y_1(\boldsymbol{Q}_{m+1},\ldots,\boldsymbol{Q}_M)\\ &\leqslant \frac{1}{S}\sum_{s=1}^{S}\left(\log_2\left|\boldsymbol{I}_{N_r}+\sum_{i=m+1}^{M}\bar{P}_i\boldsymbol{H}_{\mathrm{eq},i}\left(\boldsymbol{c}_s(n)\right)\boldsymbol{Q}_i^{(l)}\boldsymbol{H}_{\mathrm{eq},i}^{\mathrm{H}}\left(\boldsymbol{c}_s(n)\right)\right|\right)+\sum_{i=m+1}^{M}\mathrm{tr}\left(\mathrm{Re}\left\{(z_1(\boldsymbol{Q}_i^{(l)}))^{\mathrm{H}}(\boldsymbol{Q}_i-\boldsymbol{Q}_i^{(l)})\right\}\right), \end{aligned} \tag{43}$$

where $z_1(\boldsymbol{Q}_i)$ is the gradient of $y_1(\boldsymbol{Q}_{m+1}^{(l)},\ldots,\boldsymbol{Q}_i,\ldots,\boldsymbol{Q}_M^{(l)})$ that can be written as

$$\begin{aligned} z_1(\boldsymbol{Q}_i) &= \frac{\partial(y_1(\boldsymbol{Q}_{m+1}^{(l)},\ldots,\boldsymbol{Q}_i,\ldots,\boldsymbol{Q}_M^{(l)}))}{\partial(\boldsymbol{Q}_i)} \\ &= \frac{(\log_2 e)\,\bar{P}_i}{S}\sum_{s=1}^{S}\Bigg(\boldsymbol{H}_{\mathrm{eq},i}^{\mathrm{T}}(\boldsymbol{c}_s(n))\Bigg(\boldsymbol{I}_{N_r}+\sum_{j=m+1,j\neq i}^{M}\bar{P}_j\boldsymbol{H}_{\mathrm{eq},j}^{*}(\boldsymbol{c}_s(n))\,\boldsymbol{Q}_j^{(l)\mathrm{T}}\boldsymbol{H}_{\mathrm{eq},j}^{\mathrm{T}}(\boldsymbol{c}_s(n)) \\ &\quad+\bar{P}_i\boldsymbol{H}_{\mathrm{eq},i}^{*}(\boldsymbol{c}_s(n))\,\boldsymbol{Q}_i^{\mathrm{T}}\boldsymbol{H}_{\mathrm{eq},i}^{\mathrm{T}}(\boldsymbol{c}_s(n))\Bigg)^{-1}\boldsymbol{H}_{\mathrm{eq},i}^{*}(\boldsymbol{c}_s(n))\Bigg). \end{aligned} \tag{44}$$

Similarly, let

$$R_{\mathrm{BD},k}=\frac{1}{L}\log_2\left|\boldsymbol{I}_{(K-k+1)}+L\alpha\boldsymbol{\Psi}_k^{\mathrm{H}}\left(\sum_{m=1}^{M}\bar{P}_m(\boldsymbol{Q}_m)\otimes\left(\boldsymbol{L}_{m,k}^{\mathrm{H}}\boldsymbol{L}_{m,k}\right)^{\mathrm{T}}\right)\boldsymbol{\Psi}_k\right|-y_2(\boldsymbol{Q}_1,\ldots,\boldsymbol{Q}_M), \tag{45}$$

where

$$y_2(\boldsymbol{Q}_1,\ldots,\boldsymbol{Q}_M)=\frac{1}{L}\log_2\left|\boldsymbol{I}_{(K-k)}+L\alpha\boldsymbol{\Psi}_{k+1}^{\mathrm{H}}\left(\sum_{m=1}^{M}\bar{P}_m(\boldsymbol{Q}_m)\otimes\left(\boldsymbol{L}_{m,k+1}^{\mathrm{H}}\boldsymbol{L}_{m,k+1}\right)^{\mathrm{T}}\right)\boldsymbol{\Psi}_{k+1}\right|. \tag{46}$$

$y_2(\boldsymbol{Q}_1,\ldots,\boldsymbol{Q}_M)$ is also a concave differentiable function in terms of $\boldsymbol{Q}_m, m=1,\ldots,M$ with the upper bound written as

$$\begin{aligned} y_2(\boldsymbol{Q}_1,\ldots,\boldsymbol{Q}_M)\leqslant&\frac{1}{L}\log_2\left|\boldsymbol{I}_{(K-k)}+L\alpha\boldsymbol{\Psi}_{k+1}^{\mathrm{H}}\left(\sum_{m=1}^{M}\bar{P}_m\big(\boldsymbol{Q}_m^{(l)}\big)\otimes\left(\boldsymbol{L}_{m,k+1}^{\mathrm{H}}\boldsymbol{L}_{m,k+1}\right)^{\mathrm{T}}\right)\boldsymbol{\Psi}_{k+1}\right| \\ &+\sum_{m=1}^{M}\mathrm{tr}\left(\mathrm{Re}\left\{\left(z_2(\boldsymbol{Q}_m^{(l)})\right)^{\mathrm{H}}(\boldsymbol{Q}_m-\boldsymbol{Q}_m^{(l)})\right\}\right), \end{aligned} \tag{47}$$

where the expression of $z_2(\boldsymbol{Q}_m)=\frac{\partial(y_2(\boldsymbol{Q}_1^{(l)},\ldots,\boldsymbol{Q}_m,\ldots,\boldsymbol{Q}_M^{(l)}))}{\partial(\boldsymbol{Q}_m)}$ is derived as follows.

For notational convenience, we let $a=L\alpha\bar{P}_m$, $\boldsymbol{T}=\boldsymbol{I}_{(K-k)}+L\alpha\boldsymbol{\Psi}_{k+1}^{\mathrm{H}}(\sum_{i=1,i\neq m}^{M}\bar{P}_i(\boldsymbol{Q}_i^{(l)})\otimes(\boldsymbol{L}_{i,k+1}^{\mathrm{H}}\boldsymbol{L}_{i,k+1})^{\mathrm{T}})\boldsymbol{\Psi}_{k+1}\in\mathbb{C}^{(K-k)\times(K-k)}$, $\boldsymbol{C}=(\boldsymbol{L}_{m,k+1}^{\mathrm{H}}\boldsymbol{L}_{m,k+1})^{\mathrm{T}}\in\mathbb{C}^{N_t(K-k)\times N_t(K-k)}$, then we have

$$y_2(\boldsymbol{Q}_1^{(l)},\ldots,\boldsymbol{Q}_m,\ldots,\boldsymbol{Q}_M^{(l)})=\frac{\log_2 e}{L}\ln\left|\boldsymbol{T}+a\boldsymbol{\Psi}_{k+1}^{\mathrm{H}}(\boldsymbol{Q}_m\otimes\boldsymbol{C})\boldsymbol{\Psi}_{k+1}\right|=g_2(\boldsymbol{Q}_m). \tag{48}$$

Define $\boldsymbol{D}(\boldsymbol{Q}_m)=\boldsymbol{K}_{N_t\times N_t(K-k)}\boldsymbol{\Psi}_{k+1}\big(\boldsymbol{T}+a\boldsymbol{\Psi}_{k+1}^{\mathrm{H}}(\boldsymbol{Q}_m\otimes\boldsymbol{C})\boldsymbol{\Psi}_{k+1}\big)^{-1}a\boldsymbol{\Psi}_{k+1}^{\mathrm{H}}\big(\boldsymbol{I}_{N_t}\otimes\boldsymbol{C}\big)\boldsymbol{K}_{N_t\times N_t(K-k)}\in\mathbb{C}^{N_t^2(K-k)\times N_t^2(K-k)}$, where $\boldsymbol{K}_{mn}=\sum_{j=1}^{n}\left(\boldsymbol{e}_j^{\mathrm{T}}\otimes\boldsymbol{I}_m\otimes\boldsymbol{e}_j\right)\in\mathbb{C}^{mn\times mn}$. Denote $\boldsymbol{D}(\boldsymbol{Q}_m)$ as a component block matrix with $N_t^2(K-k)^2$ sub-matrices written as follows:

$$\boldsymbol{D}(\boldsymbol{Q}_m)=\begin{bmatrix}\boldsymbol{E}_{1,1}(\boldsymbol{Q}_m) & \cdots & \boldsymbol{E}_{1,N_t(K-k)}(\boldsymbol{Q}_m)\\ \vdots & \ddots & \vdots\\ \boldsymbol{E}_{N_t(K-k),1}(\boldsymbol{Q}_m) & \cdots & \boldsymbol{E}_{N_t(K-k),N_t(K-k)}(\boldsymbol{Q}_m)\end{bmatrix}, \tag{49}$$

in which $\boldsymbol{E}_{p,g}(\boldsymbol{Q}_m)\in\mathbb{C}^{N_t\times N_t}$ is the sub-matrix in $\boldsymbol{D}(\boldsymbol{Q}_m)$ at pth row and qth column.

Proposition 1. $z_2(\boldsymbol{Q}_m)$ can be expressed as

$$\begin{aligned} z_2(\boldsymbol{Q}_m)=\frac{\partial\left(g_2(\boldsymbol{Q}_m)\right)}{\partial(\boldsymbol{Q}_m)}&=\left(\frac{\log_2 e}{L}\sum_{i=1}^{N_t(K-k)}\boldsymbol{E}_{i,i}(\boldsymbol{Q}_m)\right)^{\mathrm{T}}\\ &=\frac{\log_2 e}{L}\sum_{i=1}^{N_t(K-k)}\boldsymbol{E}_{i,i}^{\mathrm{T}}(\boldsymbol{Q}_m). \end{aligned} \tag{50}$$

Proof. Please see Appendix C.

Algorithm 1 SCA Algorithm for solving problem (40)

Initialization: $\boldsymbol{Q}_m^{(0)}, m = 1, \ldots, M$, $l = 0$.
repeat
  According to the given local point $\boldsymbol{Q}_m^{(l)}$, solve the convex optimization problem (52) with the solution denoted as $\boldsymbol{Q}_m^{\star(l)}$;
  Update $\boldsymbol{Q}_m^{(l+1)} = \boldsymbol{Q}_m^{\star(l)}$;
  Update $l = l + 1$;
until The fractional increase of the objective value of problem (40) is below a threshold ϵ.

By replacing $y_1(\boldsymbol{Q}_{m+1}, \ldots, \boldsymbol{Q}_M)$ in (41) with its global upper bound in (43), and $y_2(\boldsymbol{Q}_{m+1}, \ldots, \boldsymbol{Q}_M)$ in (45) with its global upper bound in (47), $R_{\mathrm{PT},m,\mathrm{sample}}$ and $R_{\mathrm{BD},k}$ in (40c) and (40d) can be accordingly replaced with their lower bounds $R_{\mathrm{PT},m,\mathrm{sample,low}}$ and $R_{\mathrm{BD},k,\mathrm{low}}$. Then the optimization problem is given as

$$\max_{\substack{\boldsymbol{Q}_m,\\ m=1,\ldots,M}} \frac{1}{S}\sum_{s=1}^{S}\left(\log_2\left|\boldsymbol{I}_{N_r} + \sum_{m=1}^{M}\bar{P}_m\boldsymbol{H}_{\mathrm{eq},m}\left(\boldsymbol{c}_s(n)\right)\boldsymbol{Q}_m\boldsymbol{H}_{\mathrm{eq},m}^{\mathrm{H}}\left(\boldsymbol{c}_s(n)\right)\right|\right) \tag{51a}$$

$$\text{s.t.} \quad \frac{1}{L}\log_2\left|\boldsymbol{I}_K + L\alpha\boldsymbol{\Psi}_1^{\mathrm{H}}\left(\sum_{m=1}^{M}\bar{P}_m\boldsymbol{Q}_m\otimes\left(\boldsymbol{L}_{m,1}^{\mathrm{H}}\boldsymbol{L}_{m,1}\right)^{\mathrm{T}}\right)\boldsymbol{\Psi}_1\right| \geqslant r_{\mathrm{BD}}, \tag{51b}$$

$$R_{\mathrm{PT},m,\mathrm{sample,low}} \geqslant r_s, m \in \mathcal{P}, \tag{51c}$$

$$R_{\mathrm{BD},k,\mathrm{low}} \geqslant r_c, k \in \mathcal{B}, \tag{51d}$$

$$\mathrm{tr}\left(\boldsymbol{Q}_m\right) \leqslant 1, \boldsymbol{Q}_m \succeq 0, \forall m. \tag{51e}$$

For the SCA algorithm to converge, a feasible initialization is needed, which, however, is difficult to obtain for the considered problem. Fortunately, according to [39], feasible point pursuit SCA algorithm can be used to tackle this problem. To this end, we add slack variables $\boldsymbol{v} = [v_1, v_2]^{\mathrm{T}} \in \mathbb{R}^2$ to maintain feasibility, as well as a penalty μ to let the slacks be used sparingly, leading to the following problem:

$$\max_{\substack{\boldsymbol{Q}_m,\boldsymbol{v}\in\mathbb{R}^2,\\ m=1,\ldots,M}} \frac{1}{S}\sum_{s=1}^{S}\left(\log_2\left|\boldsymbol{I}_{N_r} + \sum_{m=1}^{M}\bar{P}_m\boldsymbol{H}_{\mathrm{eq},m}\left(\boldsymbol{c}_s(n)\right)\boldsymbol{Q}_m\boldsymbol{H}_{\mathrm{eq},m}^{\mathrm{H}}\left(\boldsymbol{c}_s(n)\right)\right|\right) - \mu\left\|\boldsymbol{v}\right\| \tag{52a}$$

$$\text{s.t.} \quad \frac{1}{L}\log_2\left|\boldsymbol{I}_K + L\alpha\boldsymbol{\Psi}_1^{\mathrm{H}}\left(\sum_{m=1}^{M}\bar{P}_m\boldsymbol{Q}_m\otimes\left(\boldsymbol{L}_{m,1}^{\mathrm{H}}\boldsymbol{L}_{m,1}\right)^{\mathrm{T}}\right)\boldsymbol{\Psi}_1\right| \geqslant r_{\mathrm{BD}}, \tag{52b}$$

$$R_{\mathrm{PT},m,\mathrm{sample,low}} \geqslant r_s - v_1,\ m \in \mathcal{P}, \tag{52c}$$

$$R_{\mathrm{BD},k,\mathrm{low}} \geqslant r_c - v_2,\ k \in \mathcal{B}, \tag{52d}$$

$$\mathrm{tr}\left(\boldsymbol{Q}_m\right) \leqslant 1,\ \boldsymbol{Q}_m \succeq 0,\ \forall m, \tag{52e}$$

$$v_1 \geqslant 0,\ v_2 \geqslant 0, \tag{52f}$$

where $\mu \gg 1$ is the penalty that obliges the slack variables toward zero. With the given local point $\boldsymbol{Q}_m^{(l)}$, Eqs. (52c) and (52d) are convex constraints and problem (52) is convex that can be effectively solved by CVX or other software tools [40].

Note that at least a lower bound for the optimal objective value of problem (40) can be achieved by solving problem (52), for the global lower bound in (52c) and (52d). Therefore, by iteratively optimizing (52) with the local point $\boldsymbol{Q}_m^{(l)}$ updated in each iteration, problem (40) can be efficiently solved and we summarize the process in Algorithm 1.

Let $R_{\mathrm{PT,sample}}^{(l)}$ denote the corresponding optimal value of problem (40) at the l-th iteration with the precoding matrix obtained according to Algorithm 1. The following result can be given.

Lemma 3. The average sum primary communication rate $R_{\mathrm{PT,sample}}^{(l)}$ provided by Algorithm 1 is monotonically non-decreasing, i.e., $R_{\mathrm{PT,sample}}^{(l)} \geqslant R_{\mathrm{PT,sample}}^{(l-1)}, \forall l \geqslant 1$. Furthermore, the sequence $\{\boldsymbol{Q}_m^{\star(l)}\}, l = 1, 2, \ldots,$ converges to a point that satisfies the KKT (Karush-Kuhn-Tucker) optimality conditions for the original non-convex problem (40).

Proof. Lemma 3 directly follows from [30, Proposition 3], by using the fact that the lower bound in (52c) and (52d) have both the same value and the same gradient as the sample average of the primary communication in (40c) and (40d) at the local point $\{\boldsymbol{Q}_m^{\star(l)}\}$ [33].

Table 2 System parameters

Parameter	Value
Path-loss exponent of the PT-AP link α_{TA}	2.7
Path-loss exponent of the PT-BD link α_{TB}	2.7
Noise power σ^2	-110 dBm
Power reflection coefficient ρ	1
Ratio between the symbol rate of the PT symbols and that of the BD symbols L	128

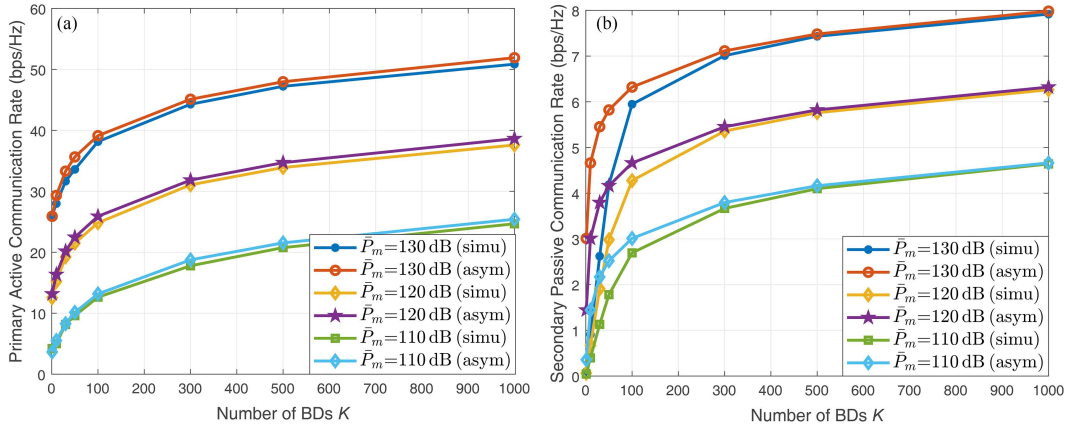

Figure 2 (Color online) (a) Asymptotic primary active communication rate versus number of BDs K in multiuser MIMO SR systems; (b) asymptotic secondary passive communication rate versus number of BDs K in multiuser MIMO SR systems.

5 Simulation results

In this section, numerical results are presented to validate the theoretical asymptotic analysis in Subsection 3.2, and evaluate the performance of our proposed solution for the general case with a finite number of BDs in Section 4. The main system parameters are listed in Table 2 unless otherwise specified.

5.1 Asymptotic analysis validation

In this subsection, the asymptotic performance in SR with a large number of BDs is illustrated according to (23) and (26) in Subsection 3.2.

Unless otherwise stated, we set $N_t = 2$, $N_r = 16$, $M = 2$, $\beta_{\mathrm{H},m} = -120$ dB, $\beta_{\mathrm{h},m} = -110$ dB, $m = 1, \ldots, M$, and $\beta_g = -20$ dB. $\bar{P}_m$, $m = 1, \ldots, M$ are assumed to be equal for all PTs. Figures 2(a) and (b) plot the sum rate of primary and secondary users versus K for both asymptotic results in (23) and (26) and the simulation results in (7) and (20), for three different transmit SNR values $\bar{P}_m$, respectively. The transmit precoding matrices $\{\boldsymbol{F}_m\}_{m=1}^M$ are set as $\frac{1}{\sqrt{N_t}}\boldsymbol{I}_{N_t}$. It can be observed from Figures 2(a) and (b) that when the number of BDs is large enough, the simulation results match quite well to the theoretical asymptotic analysis. Figure 3(a) plots $R_{\mathrm{PT}}^{\mathrm{asym}}$ versus $R_{\mathrm{BD}}^{\mathrm{asym}}$ for four different transmit SNR values $\bar{P}_m$. Note that the direct relationship between $R_{\mathrm{PT}}^{\mathrm{asym}}$ and $R_{\mathrm{BD}}^{\mathrm{asym}}$ in Figure 3(a) is obtained according to (23) and (26) by setting the same value of K. While (23) and (26) were obtained under the asymptotic assumption that $K \gg 1$, they can also be applied to the extreme case of $K = 0$, where the second term inside the logarithm of (23) and the third term inside the logarithm of (26) vanish. Therefore, Figures 2(a)–3(a) start from $K = 0$ or $R_{\mathrm{BD}}^{\mathrm{asym}} = 0$. It is observed from Figure 3(a) that once $R_{\mathrm{BD}}^{\mathrm{asym}}$ exceeds a certain threshold, $R_{\mathrm{PT}}^{\mathrm{asym}}$ increases nearly linearly with $R_{\mathrm{BD}}^{\mathrm{asym}}$, which implies that the mutualism relationship in SR can only be fully achieved when large-scale BDs are accessed. Compared with our previous work in [28] that only considers single PT, Figures 2(a)–3(a) provide more generic results considering multiple PTs. In addition, Ref. [28] only revealed the mutualism relationship between active and passive communications for the SIMO setup, while Figure 3(a) gives the results for the more general scenario in MIMO setup. Furthermore, compared with our previous work that only provides the asymptotic results based on the theoretical results, Figures 2(a) and (b) also provide numerical results to see the gap between the simulation and the analysis.

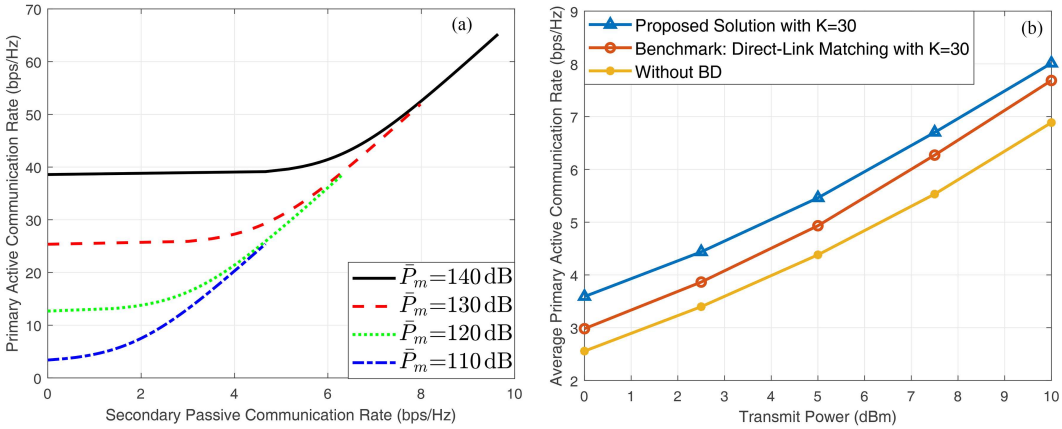

Figure 3 (Color online) (a) The asymptotic primary active versus secondary passive communication rate in multiuser MIMO SR systems; (b) sum of average primary communication rate of M PTs versus transmit power.

5.2 Scheme performance evaluation

In this subsection, we evaluate the performance of the solution proposed in Section 4. We establish a cartesian coordinate system, where the AP with $N_r = 4$ antennas is positioned at $(400\text{ m}, 0)$, and the K BDs are randomly distributed on a disk with a radius of 10 m centered at $(360, 20)$ m. Moreover, the large-scale channel gains of PTs-to-AP and PTs-to-BDs links are modeled as $\beta = \beta_0 d^{-\gamma}$, in which $\beta_0 = \left(\frac{\lambda}{4\pi}\right)^2$ represents the reference channel gain with λ being the wavelength, d is the corresponding channel link distance of PTs-to-AP or PTs-to-BDs, and γ represents the path loss exponent. Furthermore, for PT m, the large-scale channel coefficients $\beta_{h,g}^m$ of the cascaded PT-BDs-AP channels are modeled as $\beta_{h,g}^m = 0.01\beta_{m,h}$ with $\beta_{m,h}$ denoting the large-scale coefficients of PT-to-BDs channels. The maximum allowed transmit power by all PTs is equal, i.e., $P_m = P, m = 1, \ldots, M$. The subset $\mathcal{P}$ with minimum rate constraint includes all the M PTs, and the subset $\mathcal{B}$ includes one-tenth of the BDs, which are randomly chosen from all BDs. In addition, the slack penalty to eliminate dependence on feasible initialization of the SCA algorithm is $\mu = 10$. The number of samples S is 1000.

To evaluate the performance of the proposed solution in Algorithm 1, we consider a benchmark scheme named the direct-link matching precoding scheme, in which each PT directly lets the precoding matrix match the corresponding direct link while ignoring the backscattering links, i.e., $\boldsymbol{F}_m = \frac{1}{\sqrt{N_t}} \boldsymbol{V}_{\boldsymbol{H}_m} \boldsymbol{P}_m^{\frac{1}{2}}$, $m = 1, \ldots, M$, with $\boldsymbol{V}_{\boldsymbol{H}_m}$ obtained according to the (reduced) singular value decomposition (SVD) of the channel matrix $\boldsymbol{H}_m = \boldsymbol{U}_{\boldsymbol{H}_m} \boldsymbol{\Sigma}_{\boldsymbol{H}_m} \boldsymbol{V}_{\boldsymbol{H}_m}^{\mathrm{H}}$. Figure 3(b) plots the average rate of primary active communication versus the transmit power P. It can be seen that the average primary active rate increases monotonically with the transmit power P, as expected. It can also be seen that both our proposed solution and the benchmark scheme with $K = 30$ outperform the situation when there is no BD for the multipath gains provided by BDs. In addition, when the number of BDs is $K = 30$, our proposed solution based on Algorithm 1 outperforms the benchmarking direct-link matching based solution, owing to the exploitation of the additional multipaths created by passive BDs when optimizing precoding matrices.

We next investigate the effect of the number of BDs K on the average sum rate of primary and secondary communication, in which the average is taken over S independent samples and 100 independent channel realizations, with the results shown in Figures 4(a) and (b). By comparing Figures 4(a) and (b), it is observed that the sum rate of primary active communication is much higher than that of secondary passive communication. This is in line with our expectations since the symbol rate of PTs is $L = 128$ times that of the BDs. Besides, the backscattering link of one single BD is typically much weaker than each direct link due to double-hop signal attenuation. It is also observed that as the number of BDs K increases, both primary active and secondary passive communication rates increase. This thus validates our theoretical analysis in Section 3 and reveals that the mutualism relationship between primary and secondary communication rates in multiuser MIMO SR can be enhanced by using more passive devices.

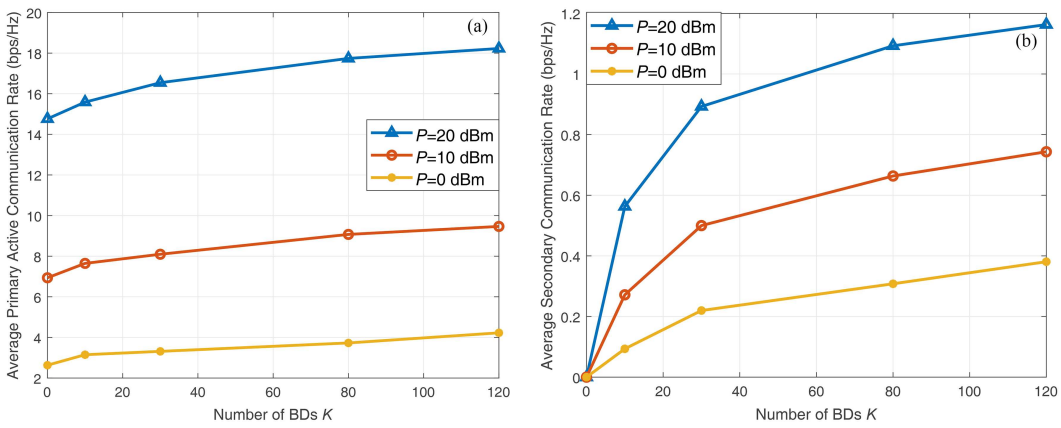

Figure 4 (Color online) Average sum rate of (a) primary communication and (b) secondary communication versus number of BDs K.

6 Conclusion

In this paper, we studied a multiuser MIMO SR system including multiple PTs and large-scale BDs. We derived the achievable rates of each PT and BD, as well as the sum rate of primary and secondary communication. Furthermore, asymptotic performance was analyzed and closed-form expressions were derived with a large number of BDs. The corresponding transmit precoding optimization problems to maximize the primary and secondary communication rate were formulated and solved, which were shown to correspond to the same optimal solution. This thus demonstrated that a win-win situation for both primary and secondary communication could be achieved with large-scale BD access. Furthermore, we formulated and solved the precoding optimization problem to maximize the sum rate of primary communication while ensuring that the sum rate of secondary communication and the individual rate for each PT and BD in the prescribed active and passive user sets satisfied the specified thresholds. Extensive simulation results were presented to demonstrate the effectiveness of our proposed algorithm.

Acknowledgements This work was supported by National Key R&D Program of China (Grant No. 2019YFB1803400).

Supporting information Appendixes A–C. The supporting information is available online at info.scichina.com and link.springer.com. The supporting materials are published as submitted, without typesetting or editing. The responsibility for scientific accuracy and content remains entirely with the authors.

References

1 Li S, Xu L D, Zhao S. 5G Internet of Things: a survey. J Indust Inf Integr, 2018, 10: 1–9
2 Shafique K, Khawaja B A, Sabir F, et al. Internet of Things (IoT) for next-generation smart systems: a review of current challenges, future trends and prospects for emerging 5G-IoT scenarios. IEEE Access, 2020, 8: 23022–23040
3 Chettri L, Bera R. A comprehensive survey on Internet of Things (IoT) toward 5G wireless systems. IEEE Int Things J, 2020, 7: 16–32
4 You X, Wang C X, Huang J, et al. Towards 6G wireless communication networks: vision, enabling technologies, and new paradigm shifts. Sci China Inf Sci, 2021, 64: 110301
5 Saad W, Bennis M, Chen M. A vision of 6G wireless systems: applications, trends, technologies, and open research problems. IEEE Netw, 2020, 34: 134–142
6 Zhang Z, Xiao Y, Ma Z, et al. 6G wireless networks: vision, requirements, architecture, and key technologies. IEEE Veh Technol Mag, 2019, 14: 28–41
7 Stankovic J A. Research directions for the Internet of Things. IEEE Int Things J, 2014, 1: 3–9
8 Hittinger E, Jaramillo P. Internet of Things: energy boon or bane? Science, 2019, 364: 326–328
9 Al-Fuqaha A, Guizani M, Mohammadi M, et al. Internet of Things: a survey on enabling technologies, protocols, and applications. IEEE Commun Surv Tut, 2015, 17: 2347–2376
10 Liang Y C, Zhang Q, Larsson E G, et al. Symbiotic radio: cognitive backscattering communications for future wireless networks. IEEE Trans Cogn Commun Netw, 2020, 6: 1242–1255
11 Yang G, Zhang Q, Liang Y C. Cooperative ambient backscatter communications for green Internet-of-Things. IEEE Int Things J, 2018, 5: 1116–1130
12 Kang X, Liang Y C, Yang J. Riding on the primary: a new spectrum sharing paradigm for wireless-powered IoT devices. IEEE Trans Wireless Commun, 2018, 17: 6335–6347
13 Yang G, Yuan D, Liang Y C, et al. Optimal resource allocation in full-duplex ambient backscatter communication networks for wireless-powered IoT. IEEE Int Things J, 2019, 6: 2612–2625
14 Hu J, Liang Y C, Pei Y. Reconfigurable intelligent surface enhanced multi-user MISO symbiotic radio system. IEEE Trans Commun, 2021, 69: 2359–2371
15 Zhang Q, Liang Y C, Poor H V. Reconfigurable intelligent surface assisted MIMO symbiotic radio networks. IEEE Trans Commun, 2021, 69: 4832–4846

16 Li X, Wang Q, Zeng M, et al. Physical-layer authentication for ambient backscatter-aided NOMA symbiotic systems. IEEE Trans Commun, 2023, 71: 2288–2303
17 Li X, Zhao M, Zeng M, et al. Hardware impaired ambient backscatter NOMA systems: reliability and security. IEEE Trans Commun, 2021, 69: 2723–2736
18 Long R, Liang Y C, Guo H, et al. Symbiotic radio: a new communication paradigm for passive Internet of Things. IEEE Int Things J, 2020, 7: 1350–1363
19 Zhang Q, Liang Y C, Yang H C, et al. Mutualistic mechanism in symbiotic radios: when can the primary and secondary transmissions be mutually beneficial? IEEE Trans Wireless Commun, 2022, 21: 8036–8050
20 Zhang Q, Liang Y C, Poor H V. Intelligent user association for symbiotic radio networks using deep reinforcement learning. IEEE Trans Wireless Commun, 2020, 19: 4535–4548
21 Chen X, Cheng H V, Shen K, et al. Stochastic transceiver optimization in multi-tags symbiotic radio systems. IEEE Int Things J, 2020, 7: 9144–9157
22 Han S, Liang Y C, Sun G. The design and optimization of random code assisted multi-BD symbiotic radio system. IEEE Trans Wireless Commun, 2021, 20: 5159–5170
23 Liu Y, Ren P, Du Q. Symbiotic communication: concurrent transmission for multi-users based on backscatter communication, In: Proceedings of International Conference on Wireless Communications and Signal Processing (WCSP), 2020. 835–839
24 Yang H, Ye Y, Liang K, et al. Energy efficiency maximization for symbiotic radio networks with multiple backscatter devices. IEEE Open J Commun Soc, 2021, 2: 1431–1444
25 Xu J, Dai Z, Zeng Y. Enabling full mutualism for symbiotic radio with massive backscatter devices. In: Proceedings of IEEE Global Communications Conference (GLOBECOM), 2021. 1–6
26 Jin N, Yang G, Liang Y C, et al. Joint beamforming and backscatter communication design for symbiotic radio networks. IEEE Int Things J, 2023, 10: 19441–19453
27 Wang J, Ding X, Zhang Q, et al. Multiple access for symbiotic radios: facilitating massive IoT connections with cellular networks. In: Proceedings of IEEE Global Communications Conference, 2022. 4812–4817
28 Xu J, Dai Z, Zeng Y. MIMO symbiotic radio with massive backscatter devices: asymptotic analysis and precoding optimization. IEEE Trans Commun, 2023, 71: 5487–5502
29 Darsena D, Gelli G, Verde F. Modeling and performance analysis of wireless networks with ambient backscatter devices. IEEE Trans Commun, 2017, 65: 1797–1814
30 Dunna M, Meng M, Wang P H, et al. SyncScatter: enabling WiFi like synchronization and range for WiFi backscatter Communication. In: Proceedings of the 18th USENIX Symposium on Networked Systems Design and Implementation, 2021. 923–937
31 Hassibi B, Hochwald B M. How much training is needed in multiple-antenna wireless links? IEEE Trans Inform Theor, 2003, 49: 951–963
32 Heath Jr R W, Lozano A. Foundations of MIMO Communication. Cambridge: Cambridge University Press, 2018
33 Zeng Y, Zhang R. Energy-efficient UAV communication with trajectory optimization. IEEE Trans Wireless Commun, 2017, 16: 3747–3760
34 Zappone A, Bjornson E, Sanguinetti L, et al. Globally optimal energy-efficient power control and receiver design in wireless networks. IEEE Trans Signal Process, 2017, 65: 2844–2859
35 Marks B R, Wright G P. Technical note — a general inner approximation algorithm for nonconvex mathematical programs. Oper Res, 1978, 26: 681–683
36 Dai Z, Li R, Xu J, et al. Rate-region characterization and channel estimation for cell-free symbiotic radio communications. IEEE Trans Commun, 2023, 71: 674–687
37 Hjϕrungnes A. Complex-valued Matrix Derivatives: with Applications in Signal Processing and Communications. Cambridge: Cambridge University Press, 2011
38 Boyd S, Vandenberghe L. Convex Optimization. Cambridge: Cambridge University Press, 2005
39 Mehanna O, Huang K, Gopalakrishnan B, et al. Feasible point pursuit and successive approximation of non-convex QCQPs. IEEE Signal Process Lett, 2015, 22: 804–808
40 Grant M, Boyd S. CVX: Matlab software for disciplined convex programming. cvxr.com/cvx